



## OPEN A novel immunomodulating peptide with potential to complement oligodeoxynucleotide-mediated adjuvanticity in vaccination strategies

Michael Agrez<sup>1,4</sup>✉, Christopher Chandler<sup>2</sup>, Kristofer J. Thurecht<sup>3,4</sup>, Nicholas L. Fletcher<sup>3,4</sup>, Feifei Liu<sup>3,4</sup>, Gayathri Subramaniam<sup>3,4</sup>, Christopher B. Howard<sup>3,4</sup>, Stephen Parker<sup>1</sup>, Darryl Turner<sup>5</sup>, Justyna Rzepecka<sup>5</sup>, Gavin Knox<sup>5</sup>, Anastasia Nika<sup>5</sup>, Andrew M. Hall<sup>5</sup>, Hayley Gooding<sup>5</sup> & Laura Gallagher<sup>5</sup>

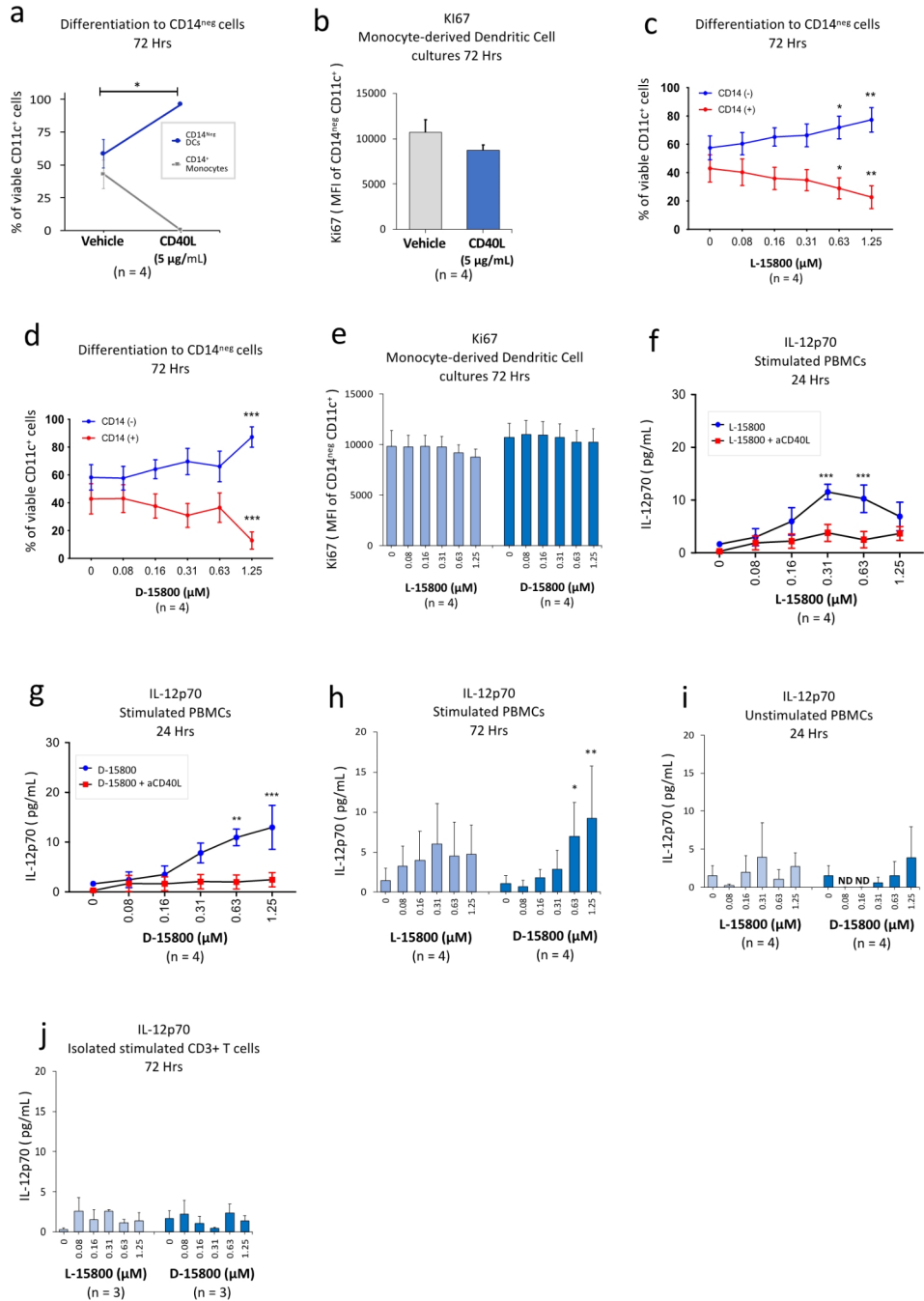
The identification of adjuvants to improve vaccination efficacy is a major unmet need. One approach is to augment the functionality of dendritic cells (DCs) by using Toll-like receptor-9 (TLR9) agonists such as cytosine-phosphate-guanine oligodeoxynucleotides (CpG ODNs) as adjuvants. Another approach is adjuvant selection based on production of bioactive interleukin-12 (IL-12). We report a D-peptide isomer, designated D-15800, that induces monocyte differentiation to the DC phenotype *in vitro* and more effectively stimulates IL-12p70 production upon T cell receptor (TCR) activation than the L-isomer. In the absence of TCR activation and either IL-12p70 or interleukin-2 production, only D-15800 activates CD4<sup>+</sup> T and natural killer cells. In the presence of CpG ODN, D-15800 synergistically enhances production of interferon-alpha (IFN- $\alpha$ ). Taken together with its biostability in human serum and depot retention upon injection, co-delivery of D-15800 with TLR9 agonists could serve to improve vaccine efficacy.

Adjuvants serve to improve the efficacy of vaccines by acting as immunostimulants and delivery system agents that enhance adaptive immunity by activating innate cells<sup>1</sup>. The most potent antigen-presenting cells are dendritic cells (DCs)<sup>2,3</sup> and increasing the functionality of DCs is a major goal in seeking to improve vaccine efficacy<sup>4</sup>. However, the outcome of antigen presentation by DCs depends on the state of DC differentiation and maturation<sup>5</sup>. Maturation of DCs is induced by DC-T cell interactions, activation of innate pattern recognition receptors called Toll-like receptors (TLRs) and inflammatory cytokine cocktails or combinations thereof<sup>6</sup>. In addition, innate natural killer (NK) cells play a role in DC-based cancer vaccines<sup>7</sup> such as recall responses to antigen re-stimulation from viral infection which facilitates durability of vaccine responses<sup>8</sup>. These recall responses are dependent on antigen-specific interleukin-2 (IL-2) from activated CD4<sup>+</sup> T cells and interleukin-12 (IL-12) produced by mature DCs<sup>9</sup> highlighting the role of adaptive and innate immunity in vaccination strategies.

*In vivo* there are two main categories of DCs: myeloid-derived or conventional DCs (cDCs) that express CD11c and plasmacytoid CD11c<sup>neg</sup> DCs (pDCs) which produce large amounts of Type I IFNs critical for initiation of antiviral immune responses<sup>10,11</sup>. Notably, pDCs do not transition from CD11c-expressing monocytes to pDCs in the presence of cytokines<sup>12,13</sup>. Given the limited availability of human cDCs, most studies that investigate cDC function rely on cells generated *in vitro* from DC precursors, i.e., CD11c<sup>+</sup>/CD14<sup>+</sup> monocytes. Exposure of peripheral blood-derived monocytes to granulocyte/macrophage-colony stimulating factor (GM-CSF) and interleukin-4 (IL-4) leads to their conversion to CD14<sup>neg</sup> monocyte-derived DCs (moDCs)<sup>14</sup> and moDCs provide a paradigm for studying cDC maturation<sup>11</sup>.

Pro-inflammatory cytokines involved in DC maturation include IL-12<sup>15,16</sup> and Type I interferon, IFN- $\alpha$ <sup>17</sup>. Survival of mature cDCs is supported by CD40 ligand (CD40L)-CD40 interactions between CD40, a membrane

<sup>1</sup>InterK Peptide Therapeutics Limited, Lane Cove West, NSW, Australia. <sup>2</sup>Auspep Pty Limited, Melbourne, Australia. <sup>3</sup>Centre for Advanced Imaging, University of Queensland, Brisbane, Australia. <sup>4</sup>Australian Institute for Bioengineering and Nanotechnology and the ARC Training Centre for Innovation in Biomedical Imaging Technologies, University of Queensland, Brisbane, Australia. <sup>5</sup>Concept Life Sciences, Edinburgh, Scotland. ✉email: michael.agrez@interk.com.au



glycoprotein on DCs<sup>18</sup> and CD40L which is expressed preferentially in activated CD4<sup>+</sup> T cells<sup>19</sup>. Both cytokines exert adjuvant effects in immunisation strategies directed against cancer<sup>20,21</sup> and viral infections<sup>22,23</sup>. In addition, IL-2, produced by CD4<sup>+</sup> Th1 helper cells<sup>24,25</sup> is a potentially useful adjuvant in vaccine strategies directed against cancer and infectious diseases in animals and humans<sup>26-29</sup>.

Amongst more recently discovered vaccine adjuvants are TLR agonists<sup>4,30</sup> that mimic conserved pathogen-associated molecular patterns (PAMPs)<sup>31,32</sup>. TLRs 3, 7, 8 and 9 are located intracellularly on endosomes and TLRs 3, 7 and 8 detect oligoribonucleotides<sup>33</sup> whereas TLR9 recognises oligodeoxynucleotide motifs present in bacterial and viral DNA<sup>4</sup>. Upon recognition of nucleic acid PAMPs in viruses and bacteria these TLRs induce production of nuclear factor (NF)-κB-mediated pro-inflammatory cytokines<sup>34</sup> that regulate cell-mediated and humoral immune responses<sup>33,35,36</sup>.

◀ **Fig. 1.** D-15800 promotes stabilisation of the DC phenotype and induces production of IL-12. Buffy coat samples were obtained from human volunteers following ethics approval. Isolated CD3<sup>+</sup> T cell cultures were stimulated with anti-CD3/anti-CD28 Dynabeads and PBMC cultures were either stimulated with anti-CD3 antibody or left unstimulated. Monocyte-derived DCs (moDCs) were prepared as described in the “Methods”. Culture durations were either 24 h or 72 h as indicated above each panel. Each tissue culture experiment was performed using triplicate wells (technical replicates). Flow cytometry for Ki67 estimation (proliferative capacity) and ELISA experiments for assessment of IL-12p70 (pg/mL) within culture supernatants were repeated either three or four times (n = experimental replicates) as indicated below each panel. All error bars represent standard error of the mean (SEM) and the effects of the L-/D-isomers compared in all experiments. Differentiation of CD14<sup>+</sup> cells to CD14<sup>neg</sup> moDCs was assessed in isolated moDC cultures exposed to recombinant rCD40L (rCD40L; 5 µg/mL) and in TCR-activated PBMC cultures exposed to L-/D-isomers in the absence/presence of neutralising anti-CD40L antibody (5 µg/mL). Flow cytometry data for Ki67 are shown as mean fluorescence intensity (MFI) and dot plots/gating strategies indicated in Supplementary Figs. S1–S3. **(a)** Differentiation of cells within moDC cultures to CD14<sup>neg</sup> cells in the presence of rCD40L after 72 h. **(b)** Ki67 expression in CD14<sup>neg</sup> cells within moDC cultures exposed to rCD40L after 72 h. **(c)** Differentiation to CD14<sup>neg</sup> cells in isolated moDC cultures exposed to L-15800 in the absence/presence of anti-CD40L antibody after 72 h. **(d)** Differentiation to CD14<sup>neg</sup> cells in isolated moDC cultures exposed to D-15800 in the absence/presence of anti-CD40L antibody after 72 h. **(e)** Ki67 expression in CD14<sup>neg</sup> cells within moDC cultures exposed to the L-/D-isomers for 72 h. **(f)** IL-12p70 production by TCR-stimulated PBMCs exposed to L-15800 in the absence/presence of anti-CD40L antibody after 24 h. **(g)** IL-12p70 production by TCR-stimulated PBMCs exposed to D-15800 in the absence/presence of anti-CD40L antibody after 24 h. **(h)** IL-12p70 production by TCR-stimulated PBMCs exposed to the L-/D-isomers for 72 h. **(i)** IL-12p70 production by non-TCR-stimulated PBMCs exposed to the L-/D-isomers for 24 h. **(j)** IL-12p70 production by TCR-stimulated CD3<sup>+</sup> T cells exposed to the L-/D-isomers for 72 h. Data for moDC cultures exposed to rCD40L were analysed by paired t-test (**a,b**). Data for moDC/PBMC/T cell cultures were analysed by means of either two-way ANOVA with Dunnett’s post-test comparing each peptide concentration with vehicle control (**c–e, h–j**) or two-way ANOVA with Sidak’s post-test comparing peptide treatment alone with peptide plus anti-CD40L antibody (**f, g**). \**P* < 0.05, \*\**P* < 0.01, \*\*\**P* < 0.001, \*\*\*\**P* < 0.0001.

In humans, TLR9 is expressed by moDCs, pDCs, B cells and natural killer (NK) cells<sup>11</sup>. Synthetic TLR9 agonists such as unmethylated cytosine-phosphate-guanine oligodeoxynucleotide (CpG ODN) mimic the function of microbial CpG ODNs<sup>37</sup> and activation of TLR9 induces signalling that culminates in transcription of Type I IFNs (IFN- $\alpha/\beta$ )<sup>4</sup>. TLR9 activation can be achieved by several classes of CpG ODNs which are based on structural attributes. CpG-A (Class A) induces production of IFN- $\alpha$  by pDCs<sup>38</sup> but not by B cells<sup>39</sup>, whereas CpG-B (Class B) directly interacts with B cells leading to secretion of IgM antibodies that is partially dependent on interleukin-6 (IL-6) expression<sup>39</sup>.

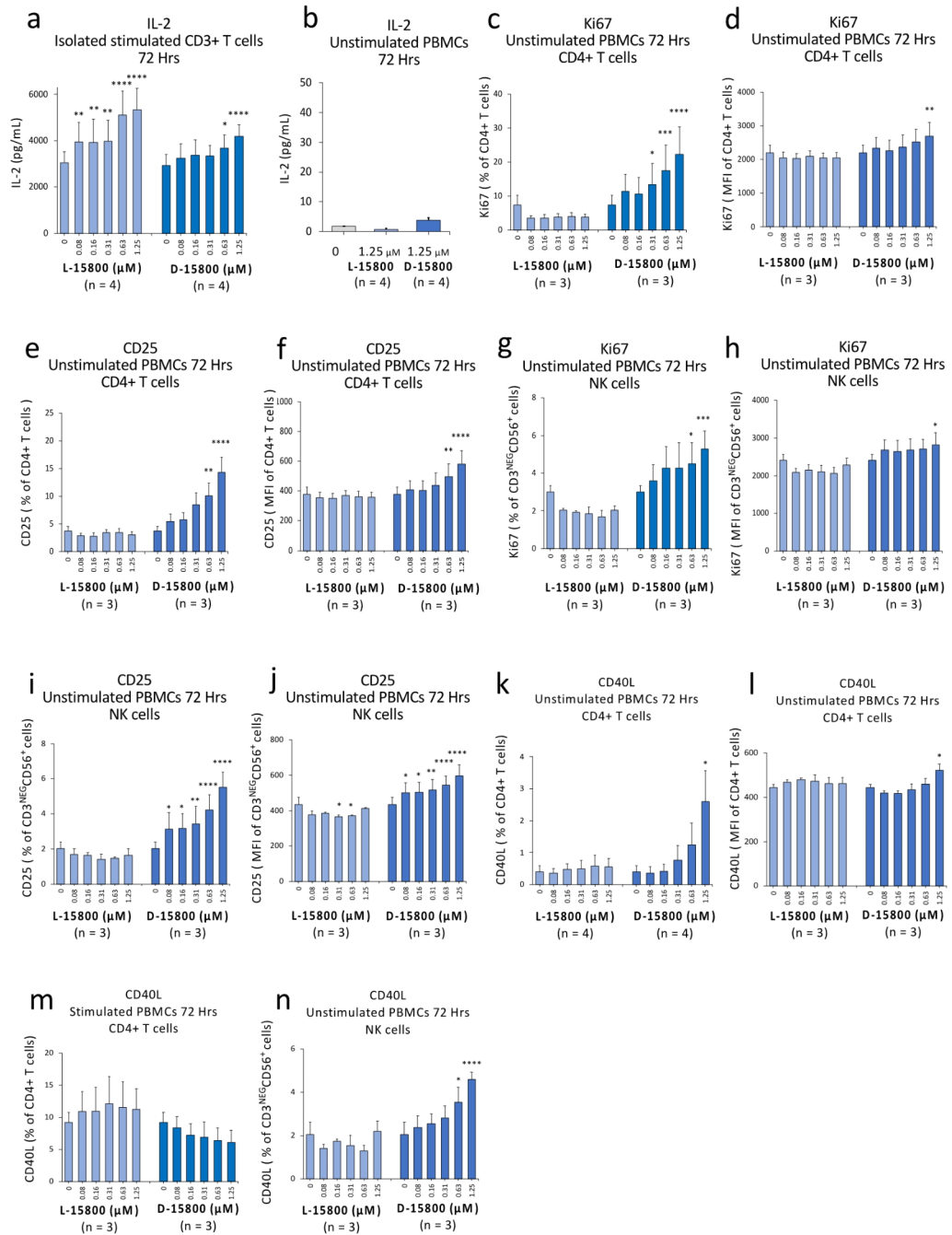
Dendritic cell persistence and antigen-presenting capacity are both dependent on CD40L-CD40 interactions<sup>40</sup> which leads to IL-12p70 production by mature as opposed to immature DCs<sup>15</sup>. While both moDCs and pDCs secrete IFN- $\alpha$  in response to TLR9 agonist, secretion of IFN- $\alpha$  by pDCs is 20–100-fold greater than by moDCs<sup>11</sup>. Furthermore, IFN- $\alpha$  produced by pDCs can promote maturation of moDCs<sup>17</sup> leading to increased IL-12p70 levels<sup>41</sup>.

We have recently reported that a 10 mer peptide sequence, RSKAKNPLYR, coupled to a fatty acid cell-penetrating moiety (CPM) stimulates IL-2 production by TCR-activated CD3<sup>+</sup> T cells but destabilises moDCs and inhibits their production of IL-12<sup>45</sup>. Amongst the branched-chain amino acids, extracellular valine has been shown to promote DC maturation which manifests as enhanced CD40L expression and IL-12p70 production<sup>43</sup>. Taken together with the importance of mature IL-12p70-producing DCs in vaccination approaches<sup>20–23</sup>, we replaced the non-R/K residues within RSKAKNPLYR with valine, i.e., RVKVKVVVVV. This was then coupled to an octa-arginine (R8) cell-penetrating moiety to facilitate solubilisation and cellular uptake given the known ability of R8 to enter the nucleus of immune cells when linked to a cargo<sup>44</sup>. Moreover, D-amino acids exhibit greater cellular uptake<sup>45</sup>. Accordingly, the conjugated peptide was synthesised as either L-/D- isomers (L-15800/D-15800, respectively) and our aim was to determine whether the isomers have immunomodulating effects on peripheral blood mononuclear cell (PBMC) subsets isolated from healthy human donors.

## Results

### D-15800 promotes stabilisation of the DC phenotype and induces production of IL-12

Dendritic cells do not express the CD14 marker that characterises monocytes<sup>14</sup>. In preliminary studies we examined the effect of recombinant CD40L (rCD40L; 5 µg/mL) on the ratio of CD14<sup>+</sup> : CD14<sup>neg</sup> cells in moDC cultures after 72 h following prior exposure of CD14<sup>+</sup> monocytes to granulocyte macrophage-colony stimulating factor (GM-CSF) and interleukin-4 (IL-4) for 7 days. Treatment with rCD40L induced near-total differentiation of cells to the CD14<sup>neg</sup> DC phenotype (Fig. 1a) which was not associated with a significant change in the proliferative capacity of the moDCs after 72 h as assessed by Ki67 expression (Fig. 1b). We next sought to determine the effect of both peptide isomers on the ratio of viable CD14<sup>+</sup> : CD14<sup>neg</sup> cells in moDC cultures. Both L-15800 (Fig. 1c) and D-15800 (Fig. 1d) induced a significant increase in the proportion of CD14<sup>neg</sup> DC cells after 72 h at the highest concentration (1.25 µM) associated with a corresponding decrease in the CD14<sup>+</sup> monocyte fraction. Moreover, at this concentration, D-15800 induced near-total differentiation of the monocyte fraction to CD14<sup>neg</sup> DCs as seen in the presence of rCD40L (Fig. 1a). To estimate whether this was associated



with expansion of the DC phenotype, the proliferative capacity of the CD14<sup>neg</sup> cells was assessed after 72 h and no significant changes were observed (Fig. 1e) as seen for cells exposed to rCD40L (Fig. 1b).

We have previously shown that CD40L induces production of IL-12p70 by TCR-stimulated PBMCs which is abolished in the presence of neutralising anti-CD40L antibody<sup>46</sup>. Given differentiation of CD14<sup>+</sup> monocytes to the CD14<sup>neg</sup> DC phenotype in the presence of either rCD40L or the peptide isomers, we examined the effects of the L-/D-peptide on IL-12p70 production by TCR-stimulated PBMCs in the absence/presence of neutralising anti-CD40L antibody (5 μg/mL). Exposure of cells to L-15800 in the absence of anti-CD40L antibody significantly enhanced production of IL-12p70 in a CD40L-dependent manner at lower peptide concentrations but this effect was decreased at higher doses at 24 h (Fig. 1f). In contrast, the D-isomer induced a dose- and CD40L-dependent increase in IL-12p70 production after 24 h (Fig. 1g) and the dose-dependent difference in IL-12p70 production between the two isomers was also reflected in PBMC cultures after 72 h (Fig. 1h). We then asked whether TCR

**◀ Fig. 2.** D-15800 enhances CD25/CD40L expression in CD4<sup>+</sup> T/ NK cells including their proliferative capacity. Buffy coat samples were obtained from human volunteers following ethics approval. Isolated CD3<sup>+</sup> T cell cultures were stimulated with anti-CD3/anti-CD28 Dynabeads and PBMC cultures either stimulated with anti-CD3 antibody to activate the TCR or left unstimulated. The culture duration in all experiments was 72 h. Each tissue culture experiment was performed using triplicate wells (technical replicates) and cell-based flow cytometry/ELISA experiments were repeated either three or four times (n = experimental replicates) as indicated below each panel. All error bars represent standard error of the mean (SEM) and the effects of the L-isomer (L-15800) and D-isomer (D-15800) compared in all experiments as indicated below each panel. Flow cytometry data are shown as either mean fluorescence intensity (MFI) or percentage values as indicated in the panels and IL-2 production assessed by means of ELISA and expressed as pg/mL. Dot plots and gating strategies are shown in Supplementary Figs. S4-S9. **(a)** IL-2 levels in supernatant from TCR-stimulated CD3<sup>+</sup> T cell cultures as assessed by ELISA. **(b)** IL-2 levels in supernatant from non-TCR-stimulated PBMC cultures. **(c)** Percentage of Ki67-expressing CD4<sup>+</sup> T cells within unstimulated PBMC cultures. **(d)** Proliferative capacity of CD4<sup>+</sup> T cells as assessed by Ki67 expression (MFI) within unstimulated PBMC cultures. **(e)** Percentage of CD25-expressing CD4<sup>+</sup> T cells within unstimulated PBMC cultures. **(f)** Expression of CD25 (MFI) in CD4<sup>+</sup> T cells within unstimulated PBMC cultures. **(g)** Percentage of Ki67-expressing NK cells within unstimulated PBMC cultures. **(h)** Proliferative capacity of NK cells as assessed by Ki67 expression (MFI) within unstimulated PBMC cultures. **(i)** Percentage of CD25-expressing NK cells within unstimulated PBMC cultures. **(j)** Expression of CD25 (MFI) in NK cells within unstimulated PBMC cultures. **(k)** Percentage of CD40L-expressing CD4<sup>+</sup> T cells within unstimulated PBMC cultures. **(l)** Expression of CD40L (MFI) in CD4<sup>+</sup> T cells within unstimulated PBMC cultures. **(m)** Percentage of CD40L-expressing CD4<sup>+</sup> T cells within TCR-stimulated PBMC cultures. **(n)** Percentage of CD40L-expressing NK cells within non-TCR-activated PBMC cultures. Flow cytometry data were analysed by two-way ANOVA with Dunnett's post-test comparing each peptide concentration with vehicle control (**c–n**). Data for IL-2 production were analysed by either two-way ANOVA with Dunnett's post-test (**a**) or one-way ANOVA with Sidak's post-test (**b**) comparing peptide isomer effects with vehicle control. \**P* < 0.05, \*\**P* < 0.01, \*\*\**P* < 0.001, \*\*\*\**P* < 0.0001.

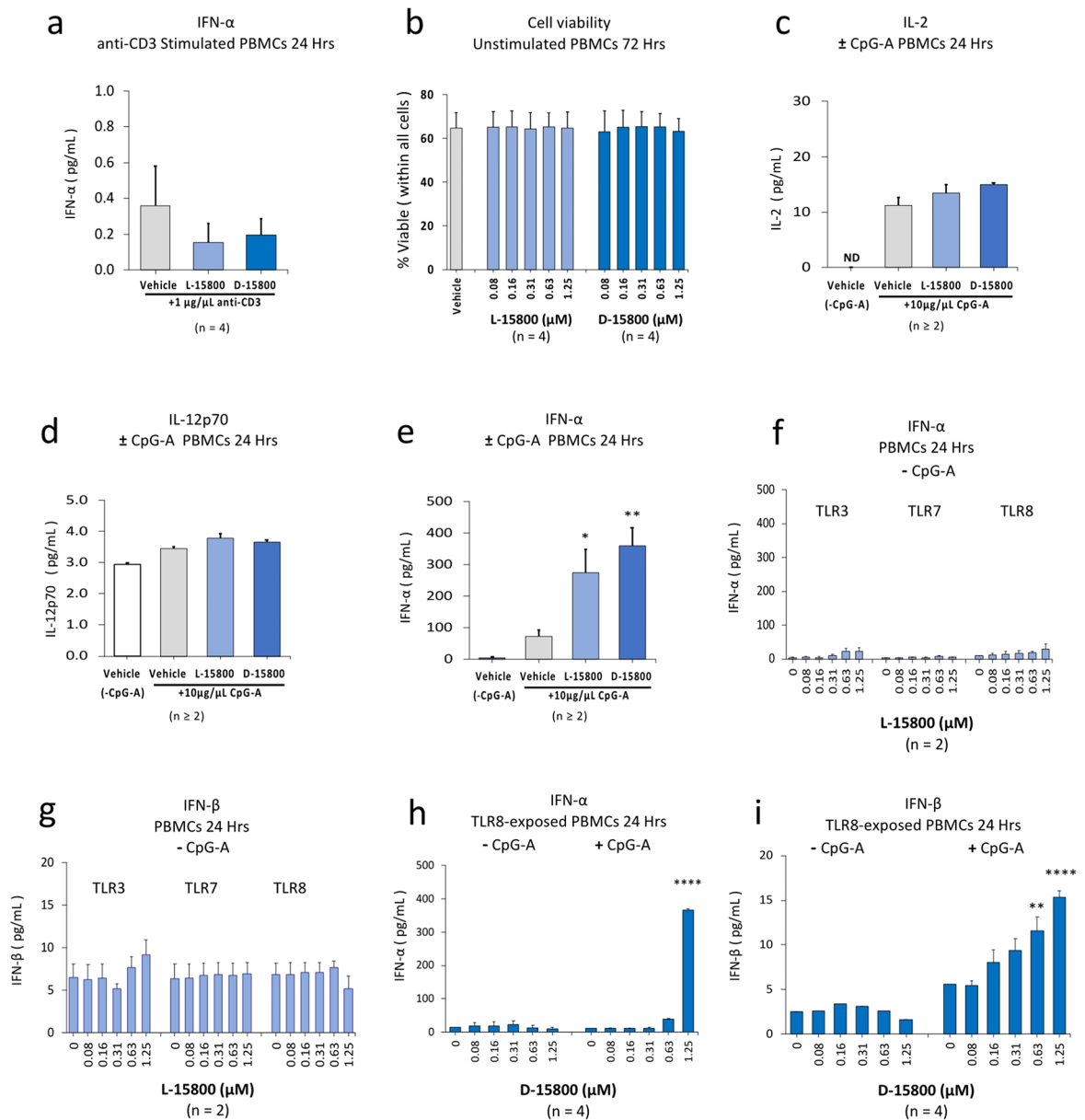
activation of PBMCs was necessary for peptide-mediated IL-12p70 responses and in the absence of anti-CD3 antibody neither L-15800 nor D-15800 induced production of IL-12p70 (Fig. 1i). Since DCs were the likely source of D-15800-induced IL-12p70, we exposed TCR-activated, isolated CD3<sup>+</sup> T cell cultures to the peptide isomers and D-15800 did not enhance IL-12p70 production after 72 h (Fig. 1j) in contrast to increased secretion of IL-12p70 by DC-containing PBMC cultures at this time point (Fig. 1h).

### D-15800 enhances CD25/CD40L expression in CD4<sup>+</sup> T/ NK cells including their proliferative capacity

T cells produce IL-2 in response to T cell receptor (TCR) activation leading to autocrine stimulation by IL-2 that induces cell proliferation<sup>47</sup> and expression of the high-affinity IL-2 receptor subunit, CD25<sup>48</sup>. However, IL-2 does not induce CD25 in freshly isolated, unstimulated, resting peripheral blood lymphocytes<sup>49</sup>. Hence, we first sought to assess the effects of both peptide isomers on IL-2 production by either anti-CD3/anti-CD28 antibody-stimulated CD3<sup>+</sup> T cell cultures or non-TCR activated PBMCs. Significant increases in IL-2 production by stimulated CD3<sup>+</sup> T cells were seen in the presence of both isomers after 72 h compared with vehicle control (Fig. 2a). However, in the absence of TCR stimulation, neither isomer induced an increase in IL-2 secretion at the highest peptide concentration (1.25 μM) in PBMC cultures after 72 h (Fig. 2b). We next sought to determine whether the isomers affect the proliferative capacity of CD4<sup>+</sup> T cells in the absence of TCR activation as assessed by expression of the nuclear proliferation marker, Ki67. Surprisingly, the proportion of Ki67-expressing CD4<sup>+</sup> T cells within unstimulated PBMC cultures was significantly enhanced in a dose-dependent manner in the presence of D-15800, but not L-15800, after 72 h (Fig. 2c). Similarly, only D-15800 induced a dose-dependent increase in the expression level (MFI) of Ki67 in CD4<sup>+</sup> T cells after 72 h (Fig. 2d). We then compared the effects of the peptide isomers on CD25 expression in CD4<sup>+</sup> T cells within unstimulated PBMC cultures. The D-15800 peptide, but not L-15800, significantly enhanced the proportion of CD25-expressing CD4<sup>+</sup> T cells after 72 h (Fig. 2e) as well as the expression level (MFI) of CD25 in a dose-dependent manner (Fig. 2f).

The proliferative capacity of NK cells is also known to be enhanced by IL-2<sup>50</sup> and given the apparent IL-2-independent effect of D-15800 on CD4<sup>+</sup> T cells, we sought to examine the effect of the L-/D- isomers on Ki67 expression in NK cells within unstimulated PBMC cultures. As seen for CD4<sup>+</sup> T cells, L-15800 did not induce an increase in the proportion of Ki67-expressing NK cells, whereas a dose-dependent increase in percentage of Ki67-expressing-NK cells was observed in the presence of D-15800 after 72 h (Fig. 2g) associated with an increase in the expression level (MFI) of Ki67 at the highest concentration (1.25 μM) (Fig. 2h). CD25 is minimally expressed in resting NK cells<sup>51</sup> and the enhanced proliferative capacity of NK cells induced by D-15800 suggested NK cell activation. We therefore examined the effect of both isomers on CD25 expression in NK cells within non-TCR-stimulated PBMC populations. The D-isomer, but not L-15800, increased the proportion of CD25-expressing NK cells (Fig. 2i) and the expression level (MFI) of CD25 after 72 h (Fig. 2j).

CD40L is one of the most potent stimulators of DC-mediated IL-12 production<sup>52–54</sup> and CD4<sup>+</sup> T helper cells proliferate poorly in response to antigen exposure without a CD40L/CD40 pathway<sup>53</sup>. Given that Ki67 expression in CD4<sup>+</sup> T cells was induced by the D-isomer in the absence of TCR activation, we then examined the effect of the L-/D-isomers on CD40L expression in CD4<sup>+</sup> T and NK cells. Importantly, IL-2-mediated signalling via its receptor complex (which includes the high-affinity CD25 subunit) modulates CD40L expression in CD4<sup>+</sup> T cells<sup>55</sup>. In light of D-15800-mediated CD25 expression in CD4<sup>+</sup> T cells in the absence of TCR activation



and IL-2 production (Fig. 2e, f and b, respectively), we first compared the effect of both isomers on CD40L expression in CD4<sup>+</sup> T cells within unstimulated PBMCs cultured for 72 h. At the highest concentration (1.25  $\mu$ M), D-15800 but not L-15800, induced a significant increase in the proportion of CD40L-expressing CD4<sup>+</sup> T cells (Fig. 2k) and in the expression level (MFI) of CD40L (Fig. 2l) which was not observed in anti-CD3-stimulated PBMC cultures (Fig. 2m). NK cells can be activated by their own CD40L<sup>56</sup>. Taken together with our finding of D-15800-mediated induction of CD25 and Ki67 expression in NK cells (Fig. 2g-j), we next sought to determine whether CD40L might play a role in activation of NK cells by the D-isomer. In unstimulated PBMC cultures, the D-isomer, but not L-15800, induced a dose-dependent increase in the proportion of CD40L-expressing NK cells after 72 h (Fig. 2n).

### The D-15800 isomer enhances CpG-A ODN-induced activation of DCs

In preliminary studies, we examined the effects of the highest peptide concentration (1.25  $\mu$ M) for both isomers on IFN- $\alpha$  production by anti-CD3-stimulated PBMCs and neither isomer enhanced the barely detectable levels of IFN- $\alpha$  after 24 h (Fig. 3a). We next examined the effect of the peptide isomers on viability of non-TCR-activated PBMCs after exposure to the compounds for 72 h and toxicity was not observed in the presence of either isomer (Fig. 3b). Microbes are an effective stimulant of IL-2 production by DCs<sup>57</sup> and taken together with our observation of D-15800-induced IL-12p70 production by TCR-activated PBMCs, we then examined the effect of both isomers on IL-2 and IL-12p70 expression when exposed to TLR9 agonist (CpG-A; 10  $\mu$ g/mL) in the absence of TCR stimulation. While a small increase in IL-2 production was observed in the presence of CpG-A alone after 24 h, this was not enhanced in the presence of either isomer at a concentration of 1.25  $\mu$ M (Fig. 3c). Similarly, in the presence of CpG-A either alone or combined with the L-/D-peptides no significant increases in IL-12p70 production were observed after 24 h (Fig. 3d). CpG-A induces IFN- $\alpha$  production by moDCs/pDCs<sup>11</sup>

◀ **Fig. 3.** The D-15800 isomer enhances CpG-A ODN-induced activation of DCs. Viability of non-TCR-activated PBMCs was assessed following exposure to the peptide isomers for 72 h. PBMCs were stimulated with either anti-CD3 antibody only or with Toll-like receptor (TLR) agonists, i.e., TLR 3 (Poly (I: C)), TLR7 (Imiquimod), TLR8 (TL8-506) and TLR9 (CpG-A ODN) for 24 h at a concentration of 10 µg/mL in the absence of TCR activation. PBMCs were exposed to TLR agonists either individually or when combined with CpG-A in the absence/presence of the L-/D-15800 isomers. Production of the cytokines IL-2, IL-12p70 and type I IFNs (IFN-α/β) was assessed by multiplex assay. The peptides were tested at concentrations either in the range of 0.08–1.25 µM or, where the dose is not indicated, only at the highest concentration, i.e., 1.25 µM. Each tissue culture experiment was performed using triplicate wells (technical replicates) and experiments repeated between two and four times because not all donor blood samples responded to TLR agonists (n = experimental replicates indicated below each panel). All error bars represent standard error of the mean (SEM). Dot plots and gating strategy for viability data are shown in the Supplementary Fig. S10. (a) IFN-α produced by anti-CD3-stimulated PBMCs exposed to either L-15800 or D-15800 at a concentration of 1.25 µM. (b) Viability of non-TCR-activated PBMCs exposed to the peptide isomers for 72 h. (c) IL-2 produced by CpG-A-stimulated PBMCs in the absence/presence of L-15800 or D-15800 at a concentration of 1.25 µM (ND = not detected). (d) IL-12p70 produced by CpG-A-stimulated PBMCs in the absence/presence of L-15800 or D-15800 at a concentration of 1.25 µM. (e) IFN-α produced by CpG-A-stimulated PBMCs in the absence/presence of L-15800 or D-15800 at a concentration of 1.25 µM. (f) IFN-α production by PBMCs stimulated with either TLR3, TLR7 or TLR8 agonist and exposed to L-15800 across the concentration range 0.08 µM – 1.25 µM. (g) IFN-β production by PBMCs stimulated with either TLR3, TLR7 or TLR8 agonist and exposed to L-15800 across the concentration range 0.08 µM – 1.25 µM. (h) IFN-α production by PBMCs stimulated either with TLR8 agonist alone or combined with TLR9 agonist and exposed to D-15800 across the concentration range 0.08 µM – 1.25 µM. (i) IFN-β production by PBMCs stimulated either with TLR8 agonist alone or combined with TLR9 agonist and exposed to D-15800 across the concentration range 0.08 µM – 1.25 µM. Data were analysed by one-way ANOVA with Holm-Sidak's post-test (a–c) or Dunnett's post-test (d) and two-way ANOVA with Dunnett's post-test (e–h) comparing each peptide concentration with vehicle control. \**P* < 0.05, \*\**P* < 0.01, \*\*\*\**P* < 0.0001.

and we next examined the effect of both isomers on IFN-α production in the presence of CpG-A. Surprisingly, a synergistic increase was observed after 24 h above that seen for CpG-ODN alone that was slightly greater in the presence of the D-isomer (Fig. 3e). Given the significant increase in IFN-α production in the combined presence of peptides and TLR9 agonist, we then sought to determine whether L-15800 also enhances type I IFN production when combined with agonists that stimulate endosomal TLRs 3, 7 and 8. However, L-15800 did not induce an increase in either IFN-α (Fig. 3f) or IFN-β production (Fig. 3g) after 24 h. TLR8 is primarily expressed in human cDCs rather than pDCs and can inhibit activation of TLR9<sup>33</sup>. We therefore sought to compare the effect of D-15800 on type I IFN production in the presence of TLR8 agonist (TL8-506; 10 µg/mL) alone and when combined with CpG-A. The D-isomer did not enhance production of IFN-α when stimulated with TLR8 agonist alone; however, a synergistic increase in secretion of IFN-α was observed in the presence of both TLR8/9 agonists (Fig. 3h) that was the same as seen in the presence of TLR9 agonist alone (Fig. 3e). Similarly, D-15800 did not induce an increase in IFN-β secretion in the presence of TLR8 alone; however, a dose-dependent increase in production of IFN-β was observed in combination with CpG-A after 24 h (Fig. 3i).

### The D-15800 isomer enhances activation of B cells in the presence of TLR9 agonist, CpG-B ODN

The TLR9 agonist, CpG-A, has little effect on IFN-α production by CD19<sup>+</sup> B cells<sup>39</sup> and we first established that neither peptide isomer affected the viability of isolated B cells (Fig. 4a). We next exposed isolated B cell cultures to L-15800/D-15800 in the presence of CpG-B (10 µg/mL) to determine whether IFN-α production could be enhanced as seen in PBMC cultures activated by CpG-A (Fig. 3e). The low level of IFN-α produced by B cells after 24 h in the presence of CpG-B alone was not altered when the TLR9 agonist was combined with either peptide isomer at the two concentrations tested, i.e., 0.63 µM and 1.25 µM (Fig. 4b). Given that CpG-B induces B cells to express IgM antibody in an IL-6-dependent manner<sup>39</sup>, we then examined the effects of the peptide isomers on IL-6 production and IgM antibody expression in B cell cultures exposed to the peptide isomers in the absence of CpG-B and neither compound enhanced IL-6 production after 24 h (Fig. 4c). However, CpG-B alone induced a marked increase in IL-6 production in the absence of peptides from 12 pg/mL (Fig. 4c) to 500 pg/mL (Fig. 4d) and this increased to 700 pg/mL in combined presence of D-15800 at the higher of the two concentrations tested, i.e., 1.25 µM, after 24 h (Fig. 4d). Consistent with the lack of effect of the peptide isomers in the absence of CpG-B on IL-6 production (Fig. 4c), neither isomer alone enhanced the expression level (MFI) of IgM (Fig. 4e). However, exposure of B cells to CpG-B alone resulted in a nearly two-fold increase in IgM and the addition of D-15800 at the highest concentration induced a further small, albeit significant, increase in IgM expression after 24 h (Fig. 4f). Similarly, the proportion of IgM-expressing B cells was not enhanced by exposure to the peptide isomers alone (Fig. 4g) but when combined with CpG-B, increases were observed in the presence of both compounds after 24 h (Fig. 4h).

### The D-15800 isomer is more stable than L-15800 in sera and forms a depot upon injection

L- and D-peptide isomers have been shown to degrade at different rates in plasma after 24 h<sup>58</sup>. Hence, we compared peptide isomer degradation over time by means of reverse phase-high performance liquid chromatography (RP-HPLC) when the compounds were exposed to either foetal bovine serum (FBS) or human serum (HS). After

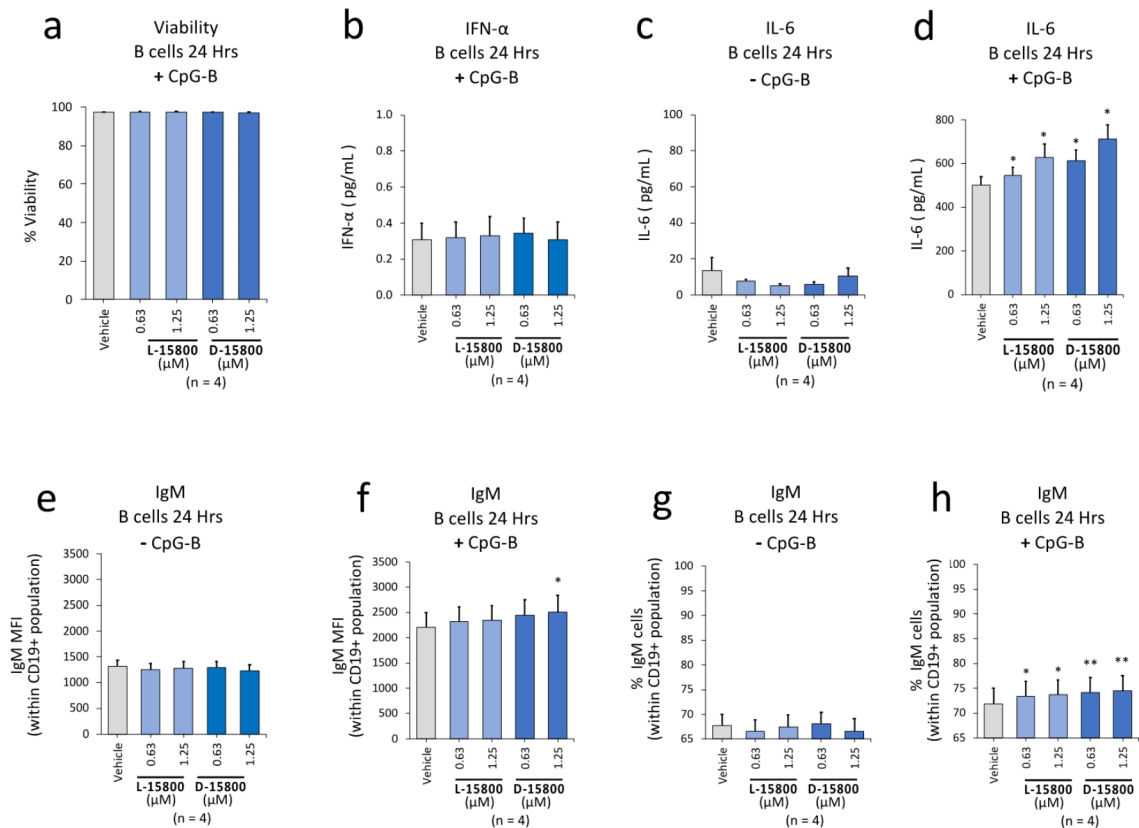


**Fig. 4.** The D-15800 isomer enhances activation of B cells in the presence of TLR9 agonist, CpG-B ODN. CD19-expressing B cells were isolated as described in the “Methods” and stimulated with TLR9 agonist (CpG-B ODN; 10 μg/mL) for 24 h either in the absence or presence of the L-/D-isomers. Production of the cytokines IFN-α and IL-6 was assessed by multiplex assay. Flow cytometry data for IgM expression are shown as either mean fluorescence intensity (MFI) or percentage values as indicated in the panels. The CpG-B concentration was 10 μg/mL and the peptides were tested at two concentrations, i.e., 0.63 μM and 1.25 μM, in all experiments as shown in the panels. Each tissue culture experiment was performed using triplicate wells (technical replicates) and experiments repeated four times (n = experimental replicates) as indicated below each panel. All error bars represent standard error of the mean (SEM). Dot plots and gating strategies are shown in the Supplementary Fig. S11. **(a)** Viability of B cells exposed to either L-15800 or D-15800 combined with CpG-B. **(b)** IFN-α secreted by CpG-B treated B cells exposed to either L-15800 or D-15800. **(c)** IL-6 secreted by B cells in the absence of CpG-B and exposed to either L-15800 or D-15800. **(d)** IL-6 secreted by B cells exposed to either L-15800 or D-15800 plus CpG-B. **(e)** Surface expression of IgM on B cells exposed to either L-15800 or D-15800 in the absence of CpG-B. **(f)** Expression level of IgM on B cells stimulated with CpG-B together with either L-15800 or D-15800. **(g)** Percentage of IgM-expressing B cells exposed to either L-15800 or D-15800 in the absence of CpG-B. **(h)** Percentage of IgM-expressing B cells treated with CpG-B together with either L-15800 or D-15800. Data were analysed by one-way ANOVA with Dunnett’s post-test comparing each peptide concentration with vehicle control. \* $P < 0.05$ , \*\* $P < 0.01$ .

48 h in the presence of FBS, 34% of L-15800 had degraded compared with 14% for D-15800 (Fig. 5a). In the presence of HS, the L-isomer was much less stable with 86% degraded after 48 h compared with 14% degradation for D-15800 (Fig. 5b). Peptides built exclusively of D amino acids persist longer in biological systems compared with L-analogues which give D-isomers a potential advantage as drugs or vaccines<sup>59</sup>. We therefore radiolabelled both constructs with <sup>64</sup>Cu and used quantitative ex vivo gamma counter analysis to compare retention of the peptide isomers within muscle 24 h after intramuscular injection in C57BL/6 mice. Retention of D-15800 at the



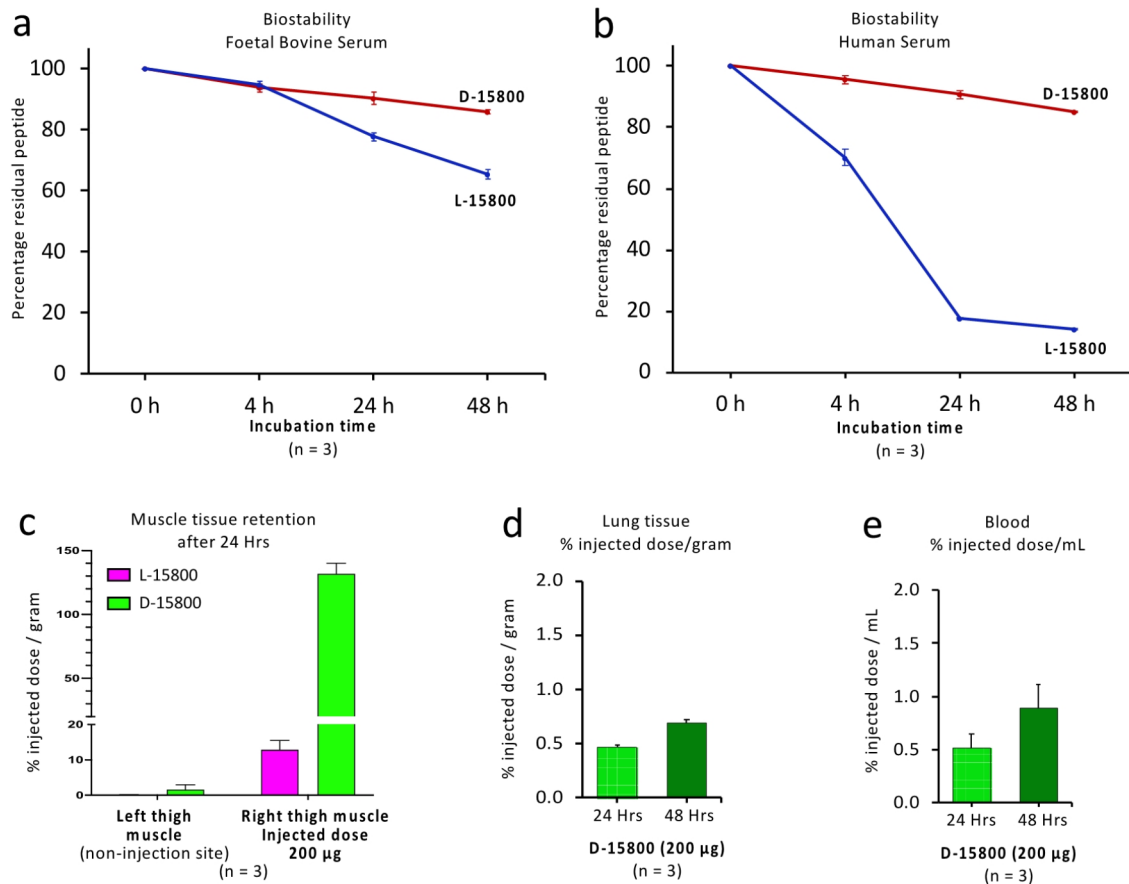


**Fig. 5.** The D-15800 isomer is more stable than L-15800 in sera and forms a depot upon injection. The stability of the L-/D-isomers dissolved in either FBS or human serum (1.0 mg/mL net) was determined by means of RP-HPLC over 48 h as described in the “Methods”. RP-HPLC-resolution data are shown in the Supplementary Fig. S12. Depot retention upon intramuscular injection of radiolabelled L-/D-isomers (200 µg) into three mice (n = experimental replicates) was assessed for both the injected thigh muscle and the contralateral thigh at 24 h and D-15800 levels compared within lung tissue and blood at 24 h and 48 h as indicated in the “Methods”. Error bars for all studies represent standard error of the mean (SEM). **(a)** Stability of the L-/D-isomers in foetal bovine serum over 48 h. **(b)** Stability of the L-/D-isomers in human serum over 48 h. **(c)** Percentage of injected dose, i.e., retention of radiolabelled  $^{64}\text{Cu}$  L-/D-isomers, in the injected thigh compared with the contralateral thigh after 24 h. **(d)** Percentage of injected  $^{64}\text{Cu}$ -labelled D-15800 in lung tissue at 24 h and 48 h. **(e)** Percentage of injected  $^{64}\text{Cu}$ -labelled D-15800 in blood at 24 h and 48 h.

injection site was 10-fold higher compared with L-15800 (Fig. 5c) and the percentage of injected D-15800 in the lung increased after 24 h (Fig. 5d) as did blood levels (Fig. 5e).

## Discussion

Herein, we have compared the biological activity of mirror image L-/D- isomers of an 18 mer peptide, RVKVKVVVVVRRRRRRRRR, designated L- and D-15800, respectively. Functional similarities between the isomers included induction of IL-2 and stimulation of TLR9-mediated signalling. However, only the D-isomer induced dose-dependent induction of IL-12p70 by DCs, activation of CD4<sup>+</sup> T and NK cells in a TCR-/cytokine-independent manner and tissue retention upon injection with greater stability in serum compared to L-15800.

Enhancing vaccine efficacy through use of adjuvants remains a major unmet need<sup>1</sup>. Vaccination against various viruses and cancers relies on the adjuvanticity provided by CpG-ODNs that stimulate TLR9-mediated signalling in DCs and B cells<sup>4,30,37,39,60–64</sup>. Cell-penetrating peptides also act as vaccine adjuvants<sup>65</sup> and L-polyarginine facilitates cellular uploading of co-administered peptide antigen without induction of antibody response against

the arginine CPM<sup>66</sup>. Given the known resistance of D-peptides to proteolysis<sup>67</sup> and their significantly greater cellular uptake compared with L-arginine isomers<sup>45</sup>, peptides built of D-amino acids have been of longstanding interest in vaccination strategies<sup>59</sup>.

The importance of mature DCs in vaccination approaches is well-recognised<sup>20–23</sup> and CD40 on DCs acts as a molecular adjuvant upon engagement with CD40L-expressing CD4<sup>+</sup> T cells which is fundamental to their helper function in cancer vaccination approaches<sup>68</sup>. This process relies on the expression of IL-12p70 by mature DCs<sup>15</sup> and in vitro production of IL-12p70 is one criterion for selection of suitable vaccine adjuvants<sup>69</sup> given benefit to cancer patients vaccinated with mature IL-12p70-producing DCs<sup>20,21</sup>. However, DC vaccination trials are only infrequently accompanied by NK cell-monitoring<sup>7</sup> which is essential given that NK responses following DC vaccination may correlate more closely with clinical outcome than T cell responses<sup>70</sup>. Not surprisingly, NK cells contribute to the efficacy of cancer vaccines<sup>71,72</sup> and increased NK cell activity has recently been observed following booster immunisation against SARS-CoV-2 Spike protein when combined with IL-12<sup>73</sup>. Of relevance to our study has been the reported finding that the amino acid, valine, is essential for DC maturation in vitro<sup>43</sup>. Accordingly, the rationale of our study was to investigate the effects of a polyarginine-linked cargo, comprising valine residues, on immunomodulation relevant to improving vaccine efficacy.

The optimal cationic cell-penetrating polyarginine sequences are either R8 or R9<sup>74</sup>. Importantly, R9 does not enhance production of either IL-2 or IL-12p70<sup>46</sup>. Our findings support the hypothesis that a valine-containing peptide cargo linked to polyarginines can promote differentiation of CD14<sup>+</sup> monocytes to the CD14<sup>neg</sup> DC phenotype. This is supported by the near-total differentiation of monocytes to the CD14<sup>neg</sup> DC phenotype accompanied by CD40L-dependent IL-12p70 production by TCR-activated PBMCs in the presence of D-15800. Importantly, IL-12p70 was not induced in the absence of DC engagement with TCR-activated CD3<sup>+</sup> T cells. In contrast, a non-valine containing cargo peptide, RSKAKNPLYR linked to R8 (designated IK14800), does not promote differentiation of monocytes to CD14<sup>neg</sup> cells and exposure of isolated CD3<sup>+</sup> T cells to IK14800 in the absence of DC engagement contributes to induction of IL-12p70<sup>46</sup>. A comparison between IK14800 and 15800 peptides was not undertaken in the present study because interpretation of cargo effects on IL-12 production would be confounded by IK14800-mediated production of IL-12p70 by T cells in the absence of DCs<sup>46</sup>. In contrast, the 15800 isomers do not induce activated T cells to express IL-12p70 in the absence of antigen-presenting cells (Fig. 1). Notably, addition of valine to serum-free cell growth medium induces production of IL-12p70 and increases the allostimulatory capacity of moDCs in contrast to the amino acid, leucine<sup>43</sup>. Hence, a comparison between D-15800 and a cargo in which valine is replaced by leucine may serve as a helpful control in future studies. Importantly, serum varies in its concentration of amino acids according to each lot number that may impact on DC phenotype and functionality<sup>43</sup> which underscores the importance of undertaking such comparisons in serum-free growth medium.

Expression of CD40L is the most potent stimulus in upregulating IL-12 production<sup>54</sup>. CD40L is preferentially expressed by activated CD4<sup>+</sup> T cells<sup>19</sup> and CD40 ligation on monocytes accelerates the maturation of DCs in the presence of GM-CSF/IL-4<sup>75</sup>. Full maturation of moDCs is not achieved in the absence of CD40L stimulation<sup>11</sup> and mature DCs produce IL-12p70 upon CD40 ligation in contrast to either immature or semimature DCs<sup>15</sup>. While we did not assess the effect of D-15800 on expression of CD40 in moDC cultures, peptide-induced IL-12p70 production was clearly dependent upon CD40L-CD40 interactions. In the absence of detectable IL-12p70 production in isolated, TCR-activated CD3<sup>+</sup> T cell cultures and by either CD14<sup>+</sup> monocytes or B cells, our findings suggest that DCs were the most likely source of IL-12p70 by TCR-activated PBMCs exposed to D-15800 for several reasons. Firstly, we have previously confirmed that induction of IL-12p70 secretion by PBMCs is dependent upon CD40L<sup>46</sup>. Secondly, exposure of monocyte-derived DC cultures to rCD40L is associated with near-total differentiation of CD14<sup>+</sup> monocytes to CD14<sup>neg</sup> cells consistent with the DC phenotype as was also seen in the presence of D-15800 at the highest concentration (1.25 μM). Thirdly, the dose-dependent increase in IL-12p70 production in PBMC cultures exposed to D-15800 was abolished in the presence of neutralising anti-CD40L antibody. Finally, engagement between TCR-activated, CD40L-expressing T cells and CD40-expressing DCs appeared necessary for IL-12p70 production given the inability of D-15800 to induce IL-12 in non-TCR-activated PBMC cultures (Fig. 1i).

We suggest that D-15800 serves as a co-stimulatory factor in CD40-mediated signalling by moDCs which contributes to their maturation and IL-12p70 production. Our finding that D-15800, but not L-15800, enhanced the proportion of CD40L-expressing CD4<sup>+</sup> T cells in the absence of TCR stimulation lends support to this hypothesis. It is also possible that decreased biostability of L-15800 compared with D-15800 may have contributed to differences in induction of IL-12p70 by the two isomers at early and later time points. Interestingly, in TCR-activated PBMCs exposed to D-15800, a dose-dependent reduction in CD40L-expressing CD4<sup>+</sup> T cells was seen (Fig. 2m) and we speculate that this was due to masking of flow staining detection due to interactions with CD40-expressing DCs.

Upon binding of cognate antigen to the TCR, DC maturation and cytokine production lead to effective T cell activation<sup>18</sup>. Activation of T cells is a multilayered process and early events include entry into the cell cycle and increase in expression of CD40L<sup>76</sup>. Induction of CD40L expression by activated CD4<sup>+</sup> T cells is regulated by both IL-2 and IL-12<sup>77</sup> and T cell activation is associated with expression of the high-affinity IL-2Rα (CD25) chain of the IL-2 receptor complex (IL-2R)<sup>39,40</sup>. The role of IL-2/IL-12 in CD40 signalling is highlighted by the inhibitory effect of anti-CD25 antibody on CD40L expression<sup>78</sup> and, in extended PBMC cultures up to 72 h, the dependency of CD40L expression on IL-12<sup>79</sup>. Only the D-isomer induced early activation changes in CD4<sup>+</sup> T cells as reflected in D-15800-mediated expression of CD25 and enhanced entry of CD4<sup>+</sup> T cells into the cell cycle, i.e., increased Ki67 expression. This was associated with increased CD40L expression in the absence of stimulatory effects from either IL-12, IL-2 or TCR activation (Figs. 1 and 2). CD25 is thought to be a limiting factor that determines the magnitude of the proliferative response of naïve CD4<sup>+</sup> T cells to antigenic stimuli<sup>80</sup> and IL-2R stimulation is linked to increased anti-tumour peptide vaccine efficacy<sup>81</sup>. CD25 expression is transiently increased upon

activation of T cells by antigen which enables antigen-activated T cells to be the preferential responders to IL-2<sup>80</sup>. Hence, induction of CD25 expression in non-activated T cells exposed to D-15800 could serve to prime their responsiveness to IL-2 upon TCR activation with expansion of antigen-specific T cell clones. Taken together, we suggest that D-15800 may prime CD4<sup>+</sup> T cells by regulating signalling pathways downstream from the TCR as well as enhancing CD40-mediated signalling upon activation of the TCR.

The dearth of effective vaccines against a wide range of microbes has highlighted the need for new vaccine development to enhance the quality of adaptive immune responses by efficient engagement of the innate immune system<sup>82</sup>. Crosstalk between NK cells and DCs enhances activation of both cell types in cancer vaccines<sup>71,72</sup>. The role of CD25 in IL-2-mediated proliferation of NK cells is highlighted by the inhibitory effect of anti-CD25 blocking antibody on IL-2-induced proliferation of NK cells pre-activated with IL-12 and interleukin-18<sup>83</sup>. As seen in CD4<sup>+</sup> T cells, only D-15800 enhanced CD25 and Ki67 expression in NK cells and increased the proportion of CD40L-expressing NK cells within unstimulated PBMC cultures. Given that NK cells can be directly activated in an autocrine manner by their own CD40L which results in NK cell proliferation<sup>56</sup>, we suggest that D-15800 may induce early activation changes in NK cells without help from activated DCs.

An interesting finding from our study was enhancement of only TLR9-mediated signalling in the presence of the peptide isomers leading to synergistic increases in IFN- $\alpha$  production in contrast to no effect on the other intracellular TLR family members in the presence of their respective agonists. CpG-A ODN is known to induce IFN- $\alpha$  production by moDCs and pDCs in the absence of T cell activation<sup>11</sup> and IFN- $\alpha$  produced by pDCs upon TLR9 activation induces maturation of moDCs<sup>17</sup> associated with increased IL-12p70 levels<sup>41</sup>. To add to this complexity, CD40L strongly promotes IFN- $\alpha$  production by pDCs induced by TLR9 agonists and CpG-stimulated pDCs added to moDC cultures promotes production of IL-12 in a dose-dependent fashion that is attributable to IFN- $\alpha$  secreted by pDCs<sup>84</sup>. Whether D-15800 combined with TLR9 agonist induces Type I IFN production by isolated pDC/moDC cultures remains to be determined. However, taken together our findings suggest that D-15800 activates moDCs when the TCR is stimulated and pDCs in the absence of TCR stimulation. Furthermore, D-15800-mediated IL-12p70 expression in a CD40L-dependent manner upon TCR stimulation raises the interesting possibility that IL-12p70 production in this setting could be further enhanced when combined with CpG-A ODN.

We also acknowledge several limitations of our study. For example, we have not established the mechanism(s) responsible for CpG-mediated stimulation by D-15800 nor demonstrated cellular entry of the peptide. Importantly, pDCs retain CpG ODN within endosomes for prolonged periods which promotes TLR9-mediated IFN- $\alpha$  production<sup>85</sup>. We think that valine residues within the peptide isomers do not contribute to the stimulatory effect on CpG-mediated signalling. Instead, electrostatic binding between the positively charged isomers and negatively charged CpG ODNs<sup>86</sup> appears more likely. This could enhance endosomal retention of TLR9 agonists and thus contribute to CpG ODN-mediated signalling. CpG ODNs also aggregate upon exposure to Na<sup>+</sup> ions, e.g., NaCl in culture medium, and aggregation suppresses TLR9 dimerisation which is required for downstream signalling and cytokine production<sup>87</sup>. Future studies to examine the size of CpG-ODNs in the absence/presence of peptide would be informative. While it is possible that D-15800 induces CpG ODN aggregate formation, we believe this is also unlikely given enhanced IFN- $\alpha$  production in the presence of peptides. Alternatively, the aggregating effect of Na<sup>+</sup> ions could be competitively inhibited by the polyarginine sequence comprising the CPM in the L-/D-isomers. Furthermore, we did not confirm cellular entry of D-15800 in the present study. Given that R8 can deliver an impermeable peptide cargo to the nucleus in immune cells<sup>44</sup>, both surface plasmon resonance assays and use of fluorescent organelle/pH-sensitive colocalization probes<sup>88</sup> in future studies should provide a better understanding of how D-15800 interacts with CpG ODNs and where this interaction takes place within cells. In addition, transcriptomic analyses to investigate peptide effects downstream from TLR9 may be helpful.

We have also not excluded the possibility that stimulation of TLR9 signalling may be related to enhanced TLR9 expression induced by the L-/D- peptide isomers. Whether human monocytes or macrophages express functional TLR9 remains controversial<sup>89</sup>. In the absence of infection, TLR9 expression in non-pDCs/B cells such as monocytes isolated from healthy donors should be low. For example, freshly isolated, non-activated monocytes do not contain TLR9 protein whereas differentiation to moDCs induces intracellular TLR9 expression<sup>11</sup>. Given that moDCs appear to contain comparable amounts of TLR9 protein to pDCs<sup>11</sup>, D-15800-mediated induction of TLR9 expression in moDCs remains an important unanswered question.

Further limitations of our study are that the effects of D-15800 *in vitro* that putatively may benefit vaccination strategies when used as a co-adjuvant together with TLR9 agonists were not confirmed *in vivo* or by vaccination experiments. In addition, antigen presentation and antigen-specific immunity was not evaluated. Notably, mouse models need to be considered with caution as they may not completely reveal the full spectrum of biological effects of Type I IFN that occur in the human system with respect to Type I IFN-mediated regulation of IL-12 secretion<sup>41</sup>. Species differences are highlighted by the production of 2000 pg/mL of IL-12 from murine splenocytes exposed to CpG-A after 24 h<sup>90</sup> in contrast to 3 pg/mL produced by human PBMCs exposed to CpG-A alone at equimolar concentrations after the same time-period (Fig. 3). Efforts to unravel how TLR9 signalling induced by CpG-ODN vaccine adjuvants may be enhanced by D-15800 also need to take into consideration differences in capture and handling of antigens between pDCs and cDCs<sup>91</sup> including stimulatory effects of pDCs on the ability of cDCs to present antigen to T cells<sup>92</sup>. Some of the best markers for phenotypic and functional DC maturation include CD83 expression<sup>93</sup> and IL-12p70<sup>15</sup> produced in response to antigenic stimulation and maturation of DCs correlates with their antigen-presenting capacity<sup>94</sup>. This has been elegantly demonstrated by the impairment of allostimulatory capacity of moDCs in valine-deprived culture medium with respect to CD83 expression and IL-12p70 production<sup>43</sup>. Hence, prior to *in vivo* studies, the effects of D-15800/CpG-ODN on antigen presentation and antigen-specific immunity will be assessed in mixed lymphocyte reaction (MLR)

assays using allogenic CD3<sup>+</sup> T cells and autologous T cells stimulated with synthetic peptides, respectively, co-cultured in serum-free defined growth medium.

In vitro immunisation with antigens and cytokines stimulates human B cell responses and is thought to be superior to conventional in vivo immunisation for antibody development that relies on T follicular helper (Tfh) cells for differentiation of naïve B cells into antibody-producing plasma cells<sup>95</sup>. CpG-B is known to directly interact with B cells leading to secretion of IgM antibody which is partially dependent on IL-6 expression<sup>39</sup>. However, the small but significant effects of D-15800/CpG-B on B cell activation with respect to IL-6 and IgM expression do not provide conclusive proof of enhanced activation of B cells by D-15800. Importantly, crosstalk exists between DCs and B cells. For example, cDCs participate in antigen presentation to B cells<sup>96</sup> and pDC-mediated Type I IFN/IL-6 secretion triggers differentiation of B cells into plasma cells<sup>97</sup>. Naïve B cells make up approximately 50% of the B cell population isolated from healthy donors<sup>98</sup> and express negligible amounts of TLR9<sup>99</sup>. We speculate that the small effects of peptide/CpG-B combinations on B cell activation in our study may have been due, at least in part, to the absence of T cell-DC engagement. Accordingly, sensitisation of mDCs to keyhole limpet hemocyanin (KLH) in vitro combined with autologous T follicular helper cells may yield more conclusive data on B cell-mediated antigen-specific immunity in the presence of D-15800/CpG-B<sup>95</sup> given that KLH induces IgM antibody production<sup>100</sup> and enhances DC activity<sup>101</sup>.

The 10-fold increase in depot retention after 24 h following intramuscular injection of the D-isomer in mice is unlikely to be related only to its stability in serum although we did not compare biostability of the two isomers in mouse serum over time. Both isomers include a cell-penetrating polyarginine sequence that facilitates intracellular uptake<sup>102</sup> and even one D-amino acid at the N-terminus of a protein suppresses intracellular proteasomal degradation<sup>103</sup>. Hence, differences in kinetics of intracellular degradation are more likely to be the major contributing factor for tissue retention and extended release of D-15800 over time. Given the long retention of D-15800, it will be important in future murine studies to determine whether D-15800 induces adverse local and systemic effects in murine models. Moreover, the large (72%) difference in biostability at 48 h between the two isomers in the presence of human serum has implications when considering immunisation with peptide-containing vaccines in human subjects. Immunocompromised individuals are least likely to respond to immunisation with a need for multiples doses<sup>104</sup> and incorporation of an adjuvant that promotes DC maturation in vaccination strategies may be especially helpful in such individuals.

In summary, we present a novel peptide with attributes potentially relevant to enhancing immune responses in vaccination approaches when administered together with TLR9 agonists. The depot-forming peptide promotes development of functionally mature DCs, stimulates TLR9-mediated signalling and induces early activation events in CD4<sup>+</sup> T and NK cells. Immunomodulation induced by D-15800 offers an opportunity to gain further insight into the intersecting CD40L/TLR9 signalling pathways involved in response to antigens. Toll-like receptor stimulation with CpG-ODNs enhances immune responses in vaccination approaches against cancer and viral diseases<sup>4,30,37,39,60–64</sup>. While no one adjuvant is appropriate for every antigen, incorporation of D-15800 as a co-adjuvant combined with TLR9 agonists may enhance vaccine efficacy against selected pathogens and cancers.

## Materials and methods

### Human ethics

All methods were carried out in accordance with relevant guidelines and regulations. Buffy coat samples from healthy human donors were obtained from Research Donors Limited via Cambridge BioScience. Ethics approval was granted by the Black Country Research Ethics Committee under REC reference 19/WM/0260. Informed consent for buffy coat samples was obtained from all subjects and/or their legal guardians in accordance with the Helsinki Declaration.

### Animal ethics

#### Accordance

All methods were carried out in accordance with relevant guidelines and regulations.

#### Arrive guidelines

All methods are reported in accordance with ARRIVE guidelines (<https://arriveguidelines.org>).

Peptide biodistribution studies in mice were approved by the University of Queensland Animal Ethics Committee and all studies were in accordance with guidelines of the Animal Ethics Committee of The University of Queensland (AIBN/530/15/ARC/NHMRC and 2020/AE000044) and the Australian Code for the Care and Use of Animals for Scientific Purposes.

### Peptide synthesis

All peptides were manufactured by Auspep (Melbourne, Australia). The unmodified sequence 15800 (RVKVKVVVRRRRRRRR-NH<sub>2</sub>; mass 2,430 Daltons) was assembled by solid phase, peptide synthesis using Fmoc protected amino acid building blocks on Rink AM resin. The modified sequence, NOTA-15800 (NOTA-RVKVKVVVRRRRRRRR-NH<sub>2</sub>), was prepared by activating 1,4,7-Triazacyclononane-1,4-bis-tert-butylacetate-7 acetic acid (Macrocylics, Inc, Plano TX, USA) and coupling this to the N-terminal of 15800. The D-isomer 15800 (rvkvkvvvrrrrrrrr-NH<sub>2</sub>) sequence was assembled by sequentially adding the D-isomeric form of the amino acid onto the core resin. Once assembled, all peptides were globally deprotected and cleaved from the resin liberating the crude, C-terminally amidated peptides. These were purified, and salt exchanged to an acetate counter-ion by RP-HPLC (C18) to a purity of > 95%. The product structures were confirmed by mass spectroscopy and amino acid analyses.

## In vitro cell cultures

### PBMCs

Preparations of peripheral blood mononuclear cells (PBMCs) and isolated T cells from buffy coat samples were performed using SepMate tubes, EasySep selection and enrichment kits, Lymphoprep, RoboSep Buffer, and EasySep magnets (STEMCELL Company). PBMCs were resuspended in RPMI-10 (RPMI-1640; ThermoFisher) supplemented with 10% heat inactivated Foetal Bovine Serum (LabTech), 100 U/mL penicillin, 100 µg/mL streptomycin (ThermoFisher), 2 mM L-glutamine (ThermoFisher), and 50 µM β-mercaptoethanol (ThermoFisher) at  $1 \times 10^6$  cells/mL and plated at a density of  $1 \times 10^5$  per well (100 µL) in 96-well, flat-bottom culture plates. PBMCs were tested either unstimulated or stimulated with 1 µg/mL of soluble anti-CD3 (BioLegend).

### CD3+ T cells and B cells

CD3<sup>+</sup> T cells were resuspended in complete medium as used for PBMCs at  $0.5 \times 10^6$ /mL and plated at a density of  $5 \times 10^4$  per well (100 µL) in 96-well, flat bottom culture plates. The T cells were stimulated with anti-CD3 anti-CD28 coated Dynabeads (ThermoFisher) at a 4:1 cell: bead ratio ( $1.25 \times 10^4$ /well, 50 µL volume) and PBMCs/isolated CD3<sup>+</sup> T cells cultured for either 24–72 h at 37 °C and 5% CO<sub>2</sub>. B cells were isolated from 2 mL PBMC ( $100 \times 10^6$  cells) using negative selection (Easy Sep B Cell Isolation kit, Cat. No. 17954, Lot. No. 100154757).

### CD14<sup>+</sup> monocytes and CD14<sup>neg</sup> dendritic cells (DCs)

CD14<sup>+</sup> monocytes were isolated from PBMCs (without CD16 depletion) by negative selection (Stem cell, Lot No. 17J83251) using immuno-magnetic separation. Cryopreserved PBMC (from the same donors) were used to derive monocyte-derived dendritic cells (moDCs) and CD14<sup>+</sup> cells isolated by using immune magnetic separation (positive selection) (Stem cell, Lot No. 17M86859) followed by culture in monocyte-DC differentiation medium (Miltenyi Biotec, Lot No. 5170627129) for seven days. At the end of this 7-day period the moDCs were ready for use.

### Peptide concentrations

The peptide isomers, L-15800 and D-15800, were solubilised as a 1 mM stock solution in sterile milliQ water (Lonza), Lot No. 6MB229) and added to wells at a final volume of 50 µL per well. The Peptide concentrations ranged from 0.08 to 1.25 µM. Vehicle controls in peptide-based experiments comprised 0.13% sterile milliQ water in culture medium. Monocyte, moDC, PBMCs and isolated CD3<sup>+</sup> T cell populations were exposed to different treatments comprising either each peptide isomer alone, each peptide isomer plus anti-CD40L antibody (5 µg/mL) (BioLegend, Lot No. B213441), recombinant CD40L (rCD40L; 5 µg/mL) (BioLegend, Lot No. B247427) alone or rCD40L in the presence of anti-CD40L antibody.

## In vitro assays

### ELISA

Supernatants were collected at the end of culture periods from unstimulated and stimulated PBMCs and isolated T cells and frozen prior to assessment for IL-2 (ThermoFisher, Lot No. 172346001) and IL-12p70 (ThermoFisher, Lot No. 173549001) production by ELISA. ELISA plates were read at 450 nm using an Infinite F50 (Tecan) absorbance reader and Magellan™ reader control and data analysis software.

### Flow cytometry

Cell staining was performed to determine cell viability (Flexible Viability Dye eFluor™ 780; ThermoFisher) and expression of extracellular/intracellular markers assessed using fluorescently-labelled antibodies against human proteins within different cell populations. T cells and NK cells (CD3<sup>neg</sup>CD56<sup>+</sup>) within PBMC populations were assessed for the following markers: CD4 (FITC Mab OKT4; ThermoFisher, BV421 Mab OKT4; CD25 (PE/Cy7, PerCP/Cy5.5; BioLegend); CD40L (anti-CD40L Mab, Cat. No. 310826, BioLegend). Intracellular expression of Ki67 (proliferation marker) (AF488; BioLegend) was assessed in CD4<sup>+</sup> T and NK cells according to a standard fixation and permeabilisation protocol (Cat. No. 00-5523-00, ThermoFisher). Monocytes and moDCs were stained for CD14<sup>+</sup>/CD11c. Flow cytometry data were exported as FCS files from Attune™ NxT software and analysed using FlowJo™ software.

## Toll-like receptor (TLR) agonist assays

### PBMCs

Human PBMCs were treated with test peptides for 24 h at 37 °C, 5% CO<sub>2</sub> in the presence of specific TLR agonists: TLR3 (Poly (I: C)) (Invivogen, Lot #PIW-41-05), TLR7 (Imiquimod) (Invivogen, Lot #IMQ-41-04), TLR8 agonist (TL8-506) (Invivogen, Lot #TL8-40-01) and TLR9 agonist (CpG-A ODN) (Invivogen, # tlr-2216, Lot# 6076-45-01) all at a final concentration of 10 µg/mL. At the end of the 24 h culture period supernatants were collected and assessed for IFN-α and IFN-β, IL-2 and IL-12p70 by multiplex (ThermoFisher, 5-plex, Cat. # PPX-05-MX324EX, Lot # 389448-000); 2-plex, Cat. # PPX-02-MXWCYJE, Lot # 390364-000) or ELISA (ThermoFisher, Cat.# 88-7025-88, Lot # 337114-007). In some studies cells were exposed to test peptides and TL8-506 plus CpG-A ODN (Invivogen, Cat # tlr-2216, Lot #4205-42T) (10 µg/mL each) and supernatants assessed for IFN-α/β by multiplex assay (ThermoFisher, ProcartaPlex Custom 2-plex, Lot # 267180).

### B cells

Isolated B cells were resuspended at  $5 \times 10^5$  cell/mL in RPMI-10 and 100 µL aliquots of B cells ( $5 \times 10^4$  cells/well) added to the appropriate wells of a 96-well round-bottom tissue culture plate. Cultures were treated with 100 µL combinations of test substance, vehicle, or CpG-B (ODN 2006, InvivoGen, Cat. No. tlr-2006, Lot. No.

6056-45-01). The final peptide concentration in all wells was 0.63 or 1.25  $\mu\text{M}$  IK15800 or IKD15800, 0.13% v/v  $\text{dH}_2\text{O}$ , and 10  $\mu\text{g}/\text{mL}$  CpG-B. Cells were cultured at approximately 37 °C for 24 h in a humidified atmosphere of 5%  $\text{CO}_2$ . Cell-free supernatants were recovered and stored frozen at approximately –20 °C for analysis of IFN $\alpha$  and IL-6 concentration by multiplex assay (ThermoFisher, Cat. No. PPX-02-MXNKURD, Lot. No. 398358-000). Remaining cells were analysed by flow cytometry for viability (eFluo780; ThermoFisher, Cat# 65-0865-14, Lot. 2633412) and expression of CD19 (PE; BioLegend, Cat. #392505, Lot No. B369430) and IgM (APC; ThermoFisher, Cat.No. 17-9998-42, Lot No. 2565445). Multiplex assays for PBMC and B cells exposed to TLR agonists were read using a Luminex FLEXMAP 3D Instrument System (ThermoFisher) and data analysed using xPONENT (ThermoFisher) software.

### Peptide isomer stability in sera

Non-cell-based assessment of peptide stability in serum for the carboxyamidated peptides L-15800 (L-enantiomer, RVKVKVVVVVRRRRRRRRR) and D-15800 (D-enantiomer, rvkvkvvvvrrrrrrrrr) at a concentration of 1.0 mg/mL in human serum (HS) (Sigma Aldrich Cat # H4522) and in foetal bovine serum (FBS) (Bovagen FBSAU 25-1980B) was determined at 37 °C  $\pm$  2 °C over 48 h. The results reported represent the average of three studies performed over sequential, 48-h periods. The degradation of the peptides over time was measured by reverse phase-high performance liquid chromatography (RP-HPLC) (Waters Corporation, USA) under the following conditions: Column (Phenomenex Jupiter 5  $\mu\text{m}$ , C4, 300 A), Buffer A (Milli-Q water, 0.1% TFA), Buffer B (90% ACN, 0.1% TFA), Gradient (Hold 5%B, 5 min; 5%B to 80%B, 20 min; 80%B to 100%B, 2.5 min). Peptide stability was determined by comparing the proportion of residual peptides with the starting peptide concentrations. The L-/D-isomers were clearly resolved at the base line from the absorbances associated with the two serums. The percentage and rate of degradation of L-15800 and D-15800 in both HS and FBS were determined by area under the curve (AUC) analysis of the integrated peak area at T=0 with those observed at the T=1, 4, 24 and 48 h time points.

### Biodistribution studies following intramuscular injection of peptide isomers

#### Labelling

1,4,7-Triazacyclononane-1,4,7-triacetic acid (NOTA) conjugated peptides were acquired from Auspep and reconstituted in deionised water at 10 mg/mL and used without further purification. Peptides were incubated with  $^{64}\text{CuCl}_2$  at 1000-fold excess of peptide in 0.1 M pH 5.5 ammonium acetate buffer for 45 min at 37 °C. 0.5  $\mu\text{L}$  samples of each solution were taken and mixed 1:1 with 50 mM EDTA. EDTA incubated sample or neat solution was spotted on TLC paper (Agilent iTLC-SG Glass microfiber chromatography paper impregnated with silica gel) and run with 50:50  $\text{H}_2\text{O}$ : ethanol as the eluent. Radioactivity in the TLC was then measured utilizing an Eckert and Zeigler Mini-Scan and Flow-Count (B-MS-1000 F) radio-TLC detector. Control experiments were conducted to monitor the elution profile of small molecule impurities bound to  $^{64}\text{Cu}$  ( $R_f$  0) and free  $^{64}\text{Cu}$  that was scavenged by EDTA ( $R_f$  1) for quality control. All samples showed 100% radiolabelling purity. Labelled peptides were then added to stocks of unlabelled peptide in phosphate buffered saline (PBS) to achieve a mass dose of 200  $\mu\text{g}$  peptide and approximately 3 MBq [ $^{64}\text{Cu}$ ]NOTA-peptide) per 50  $\mu\text{L}$  injection per mouse.

#### Dosing

All studies were in accordance with guidelines of the Animal Ethics Committee of The University of Queensland (2020/AE000044), and Australian Code for the Care and Use of Animals for Scientific Purposes. Mice were anaesthetised using 2% isoflurane in  $\text{O}_2$  for all injection and imaging procedures throughout. Female C57 mice (approximately 8 weeks of age) first had their upper thigh shaved with electric clippers and were then injected (29G needle, 50  $\mu\text{L}$  PBS solution [ $^{64}\text{Cu}$ ]NOTA-peptide) intramuscularly (upper thigh) with radiolabelled peptides. Activity present in the injection syringe was measured prior to dosing using a dose calibrator (Capintec CRC-25 pre-calibrated to  $^{64}\text{Cu}$  and the calculated injected dose determined from the residual after injection and used for calculation of percentage injected dose/g (%ID/g).

#### Ex vivo analyses

After 24- or 48-hours post administration mice ( $n=3$  each timepoint per compound) were sacrificed by cervical dislocation. Blood was sampled and tissues collected and cleaned of excess blood and weighed for ex vivo analysis. A PerkinElmer 2480 Automatic Gamma Counter was used to measure radioactivity in tissues. The gamma counter was calibrated using known samples of  $^{64}\text{Cu}$  and measured activity presented as %ID/g based on injected activities.

### Statistical analyses

For flow cytometry and ELISA experiments, data were tabulated in Excel (Microsoft) and graphs and statistical analysis prepared using GraphPad Prism (version 8.4.2) on a Windows Operating System. Data within groups were assumed to be normally distributed and to satisfy the homogeneity of variance criterion. Data from in vitro studies were analysed by means of either one-way or two-way ANOVA with Dunnett's post-test for peptide dose/vehicle comparisons or Sidak's post-test for multiple comparisons between groups. Single compound effects, e.g., single dose comparisons between vehicle and recombinant CD40L or peptide isomers were analysed by paired t-test. Statistical significance was assumed with  $P < 0.05$ .

### Data availability

Dot plot/gating strategies for flow cytometry studies are available in the Supplementary Information provided. All remaining raw datasets used and/or analysed during the current study are available from the corresponding author on reasonable request.

Received: 27 June 2024; Accepted: 29 October 2024

Published online: 05 November 2024

## References

- Zhao, T. et al. Vaccine adjuvants: mechanisms and platforms. *Signal. Transduct. Target. Ther.* **8**, 283 (2023).
- Fogel, M., Long, J. A., Thompson, P. J. & Upham, J. W. Dendritic cell maturation and IL-12 synthesis induced by the synthetic immune-response modifier S-28463. *J. Leukoc. Biol.* **72**, 932–938 (2002).
- Kaka, A. S., Foster, A. E., Weiss, H. E., Rooney, C. M. & Leen, A. M. Using dendritic cell maturation and IL-12 producing capacity as markers of function: a cautionary tale. *J. Immunother.* **31**, 359–369 (2008).
- Shirota, H. & Klinman, D. M. Recent progress concerning CpG DNA and its use as a vaccine adjuvant. *Expert Rev. Vaccines.* **13**, 299–312 (2014).
- Shakhar, G. et al. Stable T cell–dendritic cell interactions precede the development of both tolerance and immunity in vivo. *Nat. Immunol.* **6**, 707–714 (2005).
- Haenssle, H. et al. CD40 ligation during dendritic cell maturation reduces cell death and prevents interleukin-10-induced regression to macrophage-like monocytes. *Exp. Dermatol.* **17**, 177–187 (2008).
- Lion, E., Smits, E. L., Berneman, Z. N. & Van Tendeloo V. F. NK cells: Key to success of DC-based cancer vaccines? *Oncologist.* **17**, 1256–1270 (2012).
- Alrubayyi, A. et al. Natural killer cell responses during SARS-CoV-2 infection and vaccination in people living with HIV-1. *Sci. Rep.* **13**, 18994 (2023).
- Horowitz, A., Behrens, R. H., Okell, L., Fooks, A. R. & Riley, E. M. NK cells as effectors of acquired immune responses: Effector CD4+ T cell-dependent activation of NK cells following vaccination. *J. Immunol.* **185**, 2808–2818 (2010).
- Qu, C., Brinck-Jensen, N. S., Zang, M. & Chen, K. Monocyte-derived dendritic cells: Targets as potent antigen-presenting cells for the design of vaccines against infectious diseases. *Int. J. Infect. Dis.* **19**, 1–5 (2014).
- Hoene, V., Peiser, M. & Wanner, R. Human monocyte-derived dendritic cells express TLR9 and react directly to the CpG-A oligonucleotide D19. *J. Leukoc. Biol.* **80**, 1328–1336 (2006).
- Soto, J. A. et al. The role of dendritic cells during infections caused by highly prevalent viruses. *Front. Immunol.* **11**, 1513 (2020).
- Guiducci, C. et al. Properties regulating the nature of the plasmacytoid dendritic cell response to toll-like receptor 9 activation. *J. Exp. Med.* **203**, 1999–2008 (2006).
- Peters, J. H., Ruppert, J., Gieseler, R. K. H., Najjar, H. M. & Xu, H. Differentiation of human monocytes into CD14 negative accessory cells: Do dendritic cells derive from the monocytic lineage? *Pathobiology.* **59**, 122–126 (1991).
- Gerlach, A. M. et al. Role of CD40 ligation in dendritic cell semimaturation. *BMC Immunol.* **13**, 1–11 (2012).
- Dauer, M. et al. Mature dendritic cells derived from human monocytes within 48 hours: A novel strategy for dendritic cell differentiation from blood precursors. *J. Immunol.* **170**, 4069–4076 (2003).
- Gursel, M., Verthelyi, D. & Klinman, D. M. CpG oligodeoxynucleotides induce human monocytes to mature into functional dendritic cells. *Eur. J. Immunol.* **32**, 2617–2622 (2002).
- Elgueta, R. et al. Molecular mechanism and function of CD40/CD40L engagement in the immune system. *Immunol. Rev.* **229**, 152–172 (2009).
- Choi, H., Lee, H. J., Sohn, H. J. & Kim, T. G. CD40 ligand stimulation affects the number and memory phenotypes of human peripheral CD8+ T cells. *BMC Immunol.* **24**, 15 (2023).
- Lapenta, C., Gabriele, L. & Santini, S. M. IFN- $\alpha$ -mediated differentiation of dendritic cells for cancer immunotherapy: Advances and perspectives. *Vaccines.* **8**, 617 (2020).
- Carreno, B. M. et al. IL-12p70-producing patient DC vaccine elicits Tc1-polarized immunity. *J. Clin. Invest.* **123**, 3383–3394 (2013).
- Ye, L. et al. Type I and type III interferons differ in their adjuvant activities for influenza vaccines. *J. Virol.* **93**, 10–1128 (2019).
- Brook, B. et al. Adjuvantation of a SARS-CoV-2 mRNA vaccine with controlled tissue-specific expression of an mRNA encoding IL-12p70. *Sci. Transl. Med.* **16**, eadm845123 (2024).
- Létourneau, S., Krieg, C., Pantaleo, G. & Boyman, O. IL-2- and CD25-dependent immunoregulatory mechanisms in the homeostasis of T-cell subsets. *J. Allergy Clin. Immunol.* **123**, 758–762 (2009).
- Bachmann, M. F. & Oxenius, A. Interleukin 2: From immunostimulation to immunoregulation and back again. *EMBO Rep.* **8**, 1142–1148 (2007).
- Weinberg, A. & Merigan, T. C. Recombinant interleukin 2 as an adjuvant for vaccine-induced protection. Immunization of guinea pigs with herpes simplex virus subunit vaccines. *J. Immunol.* **140**, 294–299 (1988).
- Nunberg, J. H., Doyle, M. V., York, S. M. & York, C. J. Interleukin 2 acts as an adjuvant to increase the potency of inactivated rabies virus vaccine. *Proc. Natl. Acad. Sci. U S A.* **86**, 4240–4243 (1989).
- Khong, H. & Overwijk, W. W. Adjuvants for peptide-based cancer vaccines. *J. Immunother. Cancer.* **4**, 1–11 (2016).
- Alpatova, N. A., Avdeeva, Z. I., Nikitina, T. N. & Medunitsyn, N. V. Adjuvant properties of cytokines in vaccination. *Pharm. Chem. J.* **53**, 991–996 (2020).
- Luchner, M., Reinke, S. & Milicic, A. TLR agonists as vaccine adjuvants targeting cancer and infectious diseases. *Pharmaceutics.* **13**, 142 (2021).
- Aguilar, J. C. & Rodriguez, E. G. Vaccine adjuvants revisited. *Vaccine.* **25**, 3752–3762 (2007).
- Ishengoma, E. & Agaba, M. Evolution of toll-like receptors in the context of terrestrial ungulates and cetaceans diversification. *BMC Evol. Biol.* **17**, 1–13 (2017).
- Cervantes, J. L., Weirnerman, B., Basole, C. & Salazar, J. C. TLR8: The forgotten relative revindicated. *Cell. Mol. Immunol.* **9**, 434–438 (2012).
- Kawai, T. & Akira, S. Toll-like receptors and their crosstalk with other innate receptors in infection and immunity. *Immunity.* **34**, 637–650 (2011).
- Moser, M. & Leo, O. Key concepts in immunology. *Vaccine.* **28**, C2–C13 (2010).
- Vollmer, J. & Krieg, A. M. Immunotherapeutic applications of CpG oligodeoxynucleotide TLR9 agonists. *Adv. Drug Deliv. Rev.* **61**, 195–204 (2009).
- Yang, J. X. et al. TLR9 and STING agonists cooperatively boost the immune response to SARS-CoV-2 RBD vaccine through an increased germinal center B cell response and reshaped T helper responses. *Int. J. Biol. Sci.* **19**, 2897–2913 (2023).
- Nigar, S. & Shimosato, T. Cooperation of oligodeoxynucleotides and synthetic molecules as enhanced immune modulators. *Front. Nutr.* **6**, 140 (2019).
- Bode, C., Zhao, G., Steinhagen, F., Kinjo, T. & Klinman, D. M. CpG DNA as a vaccine adjuvant. *Expert Rev. Vaccines.* **10**, 499–511 (2011).
- Miga, A. J. et al. Dendritic cell longevity and T cell persistence is controlled by CD154-CD40 interactions. *Eur. J. Immunol.* **31**, 959–965 (2001).
- Luft, T. et al. IFN- $\alpha$  enhances CD40 ligand-mediated activation of immature monocyte-derived dendritic cells. *Int. Immunol.* **14**, 367–380 (2002).
- Agrez, M. et al. A novel lipidic peptide with potential to promote balanced effector-regulatory T cell responses. *Sci. Rep.* **12**, 11185 (2022).

43. Kakazu, E., Kanno, N., Ueno, Y. & Shimosegawa, T. Extracellular branched-chain amino acids, especially valine, regulate maturation and function of monocyte-derived dendritic cells. *J. Immunol.* **179**, 7137–7146 (2007).
44. Futaki, S. et al. Arginine-rich peptides: An abundant source of membrane-permeable peptides having potential as carriers for intracellular protein delivery. *J. Biol. Chem.* **276**, 5836–5840 (2001).
45. Wender, P. A. et al. The design, synthesis, and evaluation of molecules that enable or enhance cellular uptake: Peptoid molecular transporters. *Proc. Natl. Acad. Sci. U S A.* **97**, 13003–13008 (2000).
46. Agrez, M. et al. An immunomodulating peptide to counteract solar radiation-induced immunosuppression and DNA damage. *Sci. Rep.* **13**, 11702 (2023).
47. Bendickova, K. & Fric, J. Roles of IL-2 in bridging adaptive and innate immunity, and as a tool for cellular immunotherapy. *J. Leucoc Biol.* **108**, 427–437 (2020).
48. Busse, D. et al. Competing feedback loops shape IL-2 signaling between helper and regulatory T lymphocytes in cellular microenvironments. *Proc. Natl. Acad. Sci. U S A.* **107**, 3058–3063 (2010).
49. Shatrova, A. N. et al. Time-dependent regulation of IL-2R  $\alpha$ -chain (CD25) expression by TCR signal strength and IL-2-induced STAT5 signaling in activated human blood T lymphocytes. *PLoS ONE.* **11**, e0167215 (2016).
50. Wang, K. S., Frank, D. A. & Ritz, J. Interleukin-2 enhances the response of natural killer cells to interleukin-12 through up-regulation of the interleukin-12 receptor and STAT4. *Blood.* **95**, 3183–3190 (2000).
51. Gasteiger, G. et al. IL-2-dependent tuning of NK cell sensitivity for target cells is controlled by regulatory T cells. *J. Exp. Med.* **210**, 1167–1178 (2013).
52. Noelle, R. J. et al. A 39-kDa protein on activated helper T cells binds CD40 and transduces the signal for cognate activation of B cells. *Proc. Natl. Acad. Sci. U. S. A.* **89**, 6550–6554 (1992).
53. Kawabe, T., Matsushima, M., Hashimoto, N., Imaizumi, K. & Hasegawa, Y. CD40/CD40 ligand interactions in immune responses and pulmonary immunity. *Nagoya J. Med. Sci.* **73**, 69 (2011).
54. Bianchi, R. et al. Autocrine IL-12 is involved in dendritic cell modulation via CD40 ligation. *J. Immunol.* **163**, 2517–2521 (1999).
55. McDyer, J. F., Goletz, T. J., Thomas, E., June, C. H. & Seder, R. A. CD40 ligand/CD40 stimulation regulates the production of IFN- $\gamma$  from human peripheral blood mononuclear cells in an IL-12- and/or CD28-dependent manner. *J. Immunol.* **160**, 1701–1707 (1998).
56. Karnell, J. L., Rieder, S. A., Ettinger, R. & Kolbeck, R. Targeting the CD40-CD40L pathway in autoimmune diseases: Humoral immunity and beyond. *Adv. Drug Deliv. Rev.* **141**, 92–103 (2019).
57. Zelante, T., Fric, J., Wong Yoke Wei, A. & Ricciardi-Castagnoli, P. Interleukin-2 production by dendritic cells and its immunoregulatory functions. *Front. Immunol.* **3**, 161 (2012).
58. O'Neill, C. L., Shrimali, P. C., Clapacs, Z. E., Files, M. A. & Rudra, J. S. Peptide-based supramolecular vaccine systems. *Acta Biomater.* **133**, 153–167 (2021).
59. Seia, M. & Zisman, E. Different roles of D-amino acids in immune phenomena. *FASEB J.* **11**, 449–456 (1997).
60. Chen, W. et al. CpG-based nanovaccines for cancer immunotherapy. *Int. J. Nanomed.* **16**, 5281–5299 (2021).
61. Miles, M. A. et al. TLR9 monotherapy in immune-competent mice suppresses orthotopic prostate tumor development. *Cells.* **13**, 97 (2024).
62. Zhao, H. et al. CpG-C ODN M362 as an immunoadjuvant for HBV therapeutic vaccine reverses the systemic tolerance against HBV. *Int. J. Biol. Sci.* **18**, 154 (2022).
63. Yu, P. et al. A CpG oligodeoxynucleotide enhances the immune response to rabies vaccination in mice. *Virology.* **15**, 1–8 (2018).
64. Li, Y. & Chen, X. CpG 1018 is an effective adjuvant for influenza nucleoprotein. *Vaccines.* **11**, 649 (2023).
65. Lim, S., Koo, J. H. & Choi, J. M. Use of cell-penetrating peptides in dendritic cell-based vaccination. *Immune Netw.* **16**, 33–43 (2016).
66. Mattner, F. et al. Vaccination with poly-L-arginine as immunostimulant for peptide vaccines: Induction of potent and long-lasting T-cell responses against cancer antigens. *Cancer Res.* **62**, 1477–1480 (2002).
67. Van Regenmortel, M. H. & Muller, S. D-peptides as immunogens and diagnostic reagents. *Curr. Opin. Biotechnol.* **9**, 377–382 (1998).
68. Bullock, T. N. CD40 stimulation as a molecular adjuvant for cancer vaccines and other immunotherapies. *Cell. Mol. Immunol.* **19**, 14–22 (2022).
69. Napolitani, G., Rinaldi, A., Bertoni, F., Sallusto, F. & Lanzavecchia, A. Selected toll-like receptor agonist combinations synergistically trigger a T helper type 1-polarizing program in dendritic cells. *Nat. Immunol.* **6**, 769–776 (2005).
70. Osada, T., Clay, T., Hobeika, A., Lysterly, H. K. & Morse, M. A. NK cell activation by dendritic cell vaccine: A mechanism of action for clinical activity. *Cancer Immunol. Immunother.* **55**, 1122–1131 (2006).
71. Van Elssen, C. H., Oth, T., Germeraad, W. T., Bos, G. M. & Vanderlocht, J. Natural killer cells: The secret weapon in dendritic cell vaccination strategies. *Clin. Cancer Res.* **20**, 1095–1103 (2014).
72. Pampena, M. B. & Levy, E. M. Natural killer cells as helper cells in dendritic cell cancer vaccines. *Front. Immunol.* **6**, 13 (2015).
73. Mele, D. et al. Long-term dynamics of natural killer cells in response to SARS-CoV-2 vaccination: Persistently enhanced activity postvaccination. *J. Med. Virol.* **96**, e29585 (2024).
74. Zhou, J., Li, Y., Huang, W., Shi, W. & Qian, H. Source and exploration of the peptides used to construct peptide-drug conjugates. *Eur. J. Med. Chem.* **224**, 113712 (2021).
75. Rosenzweig, M., Jourquin, F., Tailleux, L. & Gluckman, J. C. CD40 ligation and phagocytosis differently affect the differentiation of monocytes into dendritic cells. *J. Leukoc. Biol.* **72**, 1180–1189 (2002).
76. Jaiswal, A. I., Dubey, C., Swain, S. L. & Croft, M. Regulation of CD40 ligand expression on naive CD4 T cells: A role for TCR but not co-stimulatory signals. *Int. Immunol.* **8**, 275–285 (1996).
77. Secor, E. R. Jr et al. Bromelain treatment reduces CD25 expression on activated CD4+ T cells in vitro. *Int. Immunopharmacol.* **9**, 340–346 (2009).
78. McDyer, J. F. et al. IL-2 receptor blockade inhibits late, but not early, IFN- $\gamma$  and CD40 ligand expression in human T cells: Disruption of both IL-12-dependent and-independent pathways of IFN- $\gamma$  production. *J. Immunol.* **169**, 2736–2746 (2002).
79. Lee, B. O., Haynes, L., Eaton, S. M., Swain, S. L. & Randall, T. D. The biological outcome of CD40 signaling is dependent on the duration of CD40 ligand expression: Reciprocal regulation by interleukin (IL)-4 and IL-12. *J. Exp. Med.* **196**, 693–704 (2002).
80. Abbas, A. K. The surprising story of IL-2: From experimental models to clinical application. *Am. J. Pathol.* **190**, 1776–1781 (2020).
81. Sultan, H. et al. Sustained persistence of IL-2 signaling enhances the antitumor effect of peptide vaccines through T-cell expansion and preventing PD-1 inhibition. *Cancer Immunol. Res.* **6**, 617–627 (2018).
82. Cox, A. et al. Targeting natural killer cells to enhance vaccine responses. *Trends Pharmacol. Sci.* **42**, 789–801 (2021). (2021).
83. Leong, J. W. et al. Preactivation with IL-12, IL-15, and IL-18 induces CD25 and a functional high-affinity IL-2 receptor on human cytokine-induced memory-like natural killer cells. *Biol. Blood Marrow Tr.* **20**, 463–473 (2014).
84. Ito, T., Kanzler, H., Duramad, O., Cao, W. & Liu, Y. J. Specialization, kinetics, and repertoire of type 1 interferon responses by human plasmacytoid predendritic cells. *Blood.* **107**, 2423–2431 (2006).
85. Honda, K. et al. Spatiotemporal regulation of MyD88-IRF-7 signalling for robust type-I interferon induction. *Nature.* **434**, 1035–1040 (2005).



86. Lingnau, K. et al. Poly-L-arginine synergizes with oligodeoxynucleotides containing CpG-motifs (CpG-ODN) for enhanced and prolonged immune responses and prevents the CpG-ODN-induced systemic release of pro-inflammatory cytokines. *Vaccine*. **20**, 3498–3508 (2002).
87. Matsuda, M. & Mochizuki, S. Control of A/D type CpG-ODN aggregates to a suitable size for induction of strong immunostimulant activity. *Biochem. Biophys. Rep.* **36**, 101573 (2023).
88. Méndez-Ardoy, A., Lostalé-Seijo, I. & Montenegro, J. Where in the cell is our cargo? Methods currently used to study intracellular cytosolic localisation. *Chembiochem*. **20**, 488–498 (2019).
89. Kiemer, A. K. et al. Attenuated activation of macrophage TLR9 by DNA from virulent mycobacteria. *J. Innate Immun.* **1**, 29–45 (2008).
90. Vollmer, J. et al. Characterization of three CpG oligodeoxynucleotide classes with distinct immunostimulatory activities. *Eur. J. Immunol.* **34**, 251–262 (2004).
91. Villadangos, J. A. & Young, L. Antigen-presentation properties of plasmacytoid dendritic cells. *Immunity*. **29**, 352–361 (2008).
92. Lou, Y. et al. Plasmacytoid dendritic cells synergize with myeloid dendritic cells in the induction of antigen-specific antitumor immune responses. *J. Immunol.* **178**, 1534–1541 (2007).
93. Lechmann, M., Berchtold, S., Steinkasserer, A. & Hauber, J. CD83 on dendritic cells: More than just a marker for maturation. *Trends Immunol.* **23**, 273–275 (2002).
94. Jin, Y. & ET, A. L. Antigen presentation and immune regulatory capacity of immature and mature-enriched antigen presenting (dendritic) cells derived from human bone marrow. *Hum. Immunol.* **65**, 93–103 (2004).
95. Fang, X. et al. Rapid de novo generation of antigen specific human B cells with expression of Blimp-1 and AID by in vitro immunization. *Exp. Cell. Res.* **352**, 53–62 (2017).
96. Heath, W. R., Kato, Y., Steiner, T. M. & Caminschi, I. Antigen presentation by dendritic cells for B cell activation. *Curr. Opin. Immunol.* **58**, 44–52 (2019).
97. Yang, L., Li, S., Chen, L. & Zhang, Y. Emerging roles of plasmacytoid dendritic cell crosstalk in tumor immunity. *Cancer Biol. Med.* **20**, 728 (2023).
98. Velounias, R. L. & Tull, T. J. Human B-cell subset identification and changes in inflammatory diseases. *Clin. Exp. Immunol.* **210**, 201–216 (2022).
99. Bernasconi, N. L. et al. A role for toll-like receptors in acquired immunity: Up-regulation of TLR9 by BCR triggering in naive B cells and constitutive expression in memory B cells. *Blood*. **101**, 4500–4504 (2003).
100. Morimoto, C. et al. Primary in vitro anti-KLH antibody formation by peripheral blood lymphocytes in man: Detection with a radioimmunoassay. *J. Immunol.* **127**, 514–517 (1981).
101. Presicce, P., Taddeo, A., Conti, A., Villa, M. L. & Della Bella, S. Keyhole limpet hemocyanin induces the activation and maturation of human dendritic cells through the involvement of mannose receptor. *Molec Immunol.* **45**, 1136–1145 (2008).
102. Hao, M., Zhang, L. & Chen, P. Membrane internalization mechanisms and design strategies of arginine-rich cell-penetrating peptides. *Int. J. Mol. Sci.* **23**, 9038 (2022).
103. Rabideau, A. E. & Pentelute, B. L. A d-amino acid at the N-terminus of a protein abrogates its degradation by the N-end rule pathway. *ACS Cent. Sci.* **1**, 423–430 (2015).
104. Ljungman, P. Vaccination of immunocompromised patients. *Clin. Microbiol. Infect.* **18**, 93–99 (2012).

### Author contributions

M.A. conceived the project, analysed the data and wrote the manuscript. All experiments using immune cells from healthy volunteers were conducted by J.R., G.K., D.T., A.M.H., A.N., H.G. and L.G. who also provided helpful input into interpretation of data. C.C. provided the synthesised peptides and conducted the peptide biostability studies. S.P. assisted with preparation of all Figures. N.L.F. and K.J.T. conducted the biodistribution studies assisted by F.L., G.S. and C.B.H.

### Declarations

#### Competing interests

The authors M.A. and S.P. declare competing financial interest as Executive Directors of InterK Peptide Therapeutics Limited. The remaining authors do not have any competing interests.

#### Additional information

**Supplementary Information** The online version contains supplementary material available at <https://doi.org/10.1038/s41598-024-78150-7>.

**Correspondence** and requests for materials should be addressed to M.A.

**Reprints and permissions information** is available at [www.nature.com/reprints](http://www.nature.com/reprints).

**Publisher's note** Springer Nature remains neutral with regard to jurisdictional claims in published maps and institutional affiliations.

**Open Access** This article is licensed under a Creative Commons Attribution-NonCommercial-NoDerivatives 4.0 International License, which permits any non-commercial use, sharing, distribution and reproduction in any medium or format, as long as you give appropriate credit to the original author(s) and the source, provide a link to the Creative Commons licence, and indicate if you modified the licensed material. You do not have permission under this licence to share adapted material derived from this article or parts of it. The images or other third party material in this article are included in the article's Creative Commons licence, unless indicated otherwise in a credit line to the material. If material is not included in the article's Creative Commons licence and your intended use is not permitted by statutory regulation or exceeds the permitted use, you will need to obtain permission directly from the copyright holder. To view a copy of this licence, visit <http://creativecommons.org/licenses/by-nc-nd/4.0/>.

© The Author(s) 2024